

CAPITAL UNIVERSITY OF SCIENCE AND
TECHNOLOGY, ISLAMABAD



**Non-uniform heat source/sink
and activation energy effects on
micropolar fluid in the presence
of inclined magnetic field and
thermal radiation**

by

Waqar Younas

A thesis submitted in partial fulfillment for the
degree of Master of Philosophy

in the

Faculty of Computing
Department of Mathematics

2018

Copyright © 2017 by Waqar Younas

All rights reserved. No part of this thesis may be reproduced, distributed, or transmitted in any form or by any means, including photocopying, recording, or other electronic or mechanical methods, by any information storage and retrieval system without the prior written permission of the author.

I dedicate this sincere effort to my beloved **Parents** and my elegant **Teachers** whose devotions and contributions to my life are really worthless and whose deep consideration on part of my academic career, made me consolidated and inspired me as I am upto this grade now.



CAPITAL UNIVERSITY OF SCIENCE & TECHNOLOGY
ISLAMABAD

CERTIFICATE OF APPROVAL

**Non-uniform heat source/sink and activation energy
effects on micropolar fluid in the presence of inclined
magnetic field and thermal radiation**

by

Waqar Younas

(MMT163010)

THESIS EXAMINING COMMITTEE

S. NO	Examinor	Name	Organization
(a)	External	Dr. Muhammad Yousaf	CIIT, Islamabad
(b)	Internal	Dr. Rashid Ali	CUST, Islamabad
(c)	Supervisor	Dr. Muhammad Sagheer	CUST, Islamabad

Dr. Muhammad Sagheer

Thesis Supervisor

October, 2018

Dr. Muhammad Sagheer

Head

Dept. of Mathematics

October, 2018

Dr. Muhammad Abdul Qadir

Dean

Faculty of Computing

October, 2018

Author's Declaration

I, **Waqar Younas** hereby state that my M.Phil thesis titled “**Non-uniform heat source/sink and activation energy effects on micropolar fluid in the presence of inclined magnetic field and thermal radiation**” is my own work and has not been submitted previously by me for taking any degree from Capital University of Science and Technology, Islamabad or anywhere else in the country/abroad.

At any time if my statement is found to be incorrect even after my graduation, the University has the right to withdraw my M.Phil Degree.

(Waqar Younas)

Registration No: MMT163010

Plagiarism Undertaking

I solemnly declare that research work presented in this thesis titled “*Non-uniform heat source/sink and activation energy effects on micropolar fluid in the presence of inclined magnetic field and thermal radiation*” is solely my research work with no significant contribution from any other person. Small contribution/help wherever taken has been dully acknowledged and that complete thesis has been written by me.

I understand the zero tolerance policy of the HEC and Capital University of Science and Technology towards plagiarism. Therefore, I as an author of the above titled thesis declare that no portion of my thesis has been plagiarized and any material used as reference is properly referred/cited.

I undertake that if I am found guilty of any formal plagiarism in the above titled thesis even after award of M.Phil Degree, the University reserves the right to withdraw/revoke my M.Phil degree and that HEC and the University have the right to publish my name on the HEC/University website on which names of students are placed who submitted plagiarized work.

(Waqar Younas)

Registration No: MMT163010

Acknowledgements

All praises to Almighty **Allah**, the Creator of all the creatures in the universe, who has created us in the structure of human beings as the best creature. Many thanks to Him, who created us as a muslim and blessed us with knowledge to differentiate between right and wrong. Many many thanks to Him as he blessed us with the Holy Prophet, **Hazrat Muhammad (Sallallahu Alaihay Wa'alihi wasalam)** for Whom the whole universe is created. He (Sallallahu Alaihay Wa'alihi wasalam) brought us out of darkness and enlightened the way to heaven. I express my heartfelt gratitude to my supervisor **Dr. Muhammad Sagheer** for his passionate interest, superb guidance and inexhaustible inspiration throughout this investigation. His textual and verbal criticism enabled me in formatting this manuscript. I would like to acknowledge CUST for providing me such a favourable environment to conduct this research. I especially deem to express my unbound thanks to **Dr. Shafqat Hussain** for his excellent supervision merged with his affection and obligation, without him I would have not been able to commence this current research study.

I would also like to thank especially to the PhD scholar **Mr. Sajid Shah** for his valuable guidance, suggestions and comments in the completion of my thesis. My heartiest and sincere salutations to my Parents, who put their unmatched efforts in making me a good human being.

May Almighty Allah shower His choicest blessings and prosperity on all those who helped me in any way during the completion of my thesis.

Abstract

In this thesis the effects of inclined magnetic field, Soret and Dufour numbers and activation energy on the two-dimensional hydromagnetic mixed convective heat and mass transfer flow of a micropolar fluid over a stretching sheet embedded in a non-Darcian porous medium with thermal radiation, have been discussed in detail. The formulated highly non linear equations for the above mentioned flow are converted into first order ODEs. The shooting method is used to solve the BVP by using the computational software MATLAB. A built-in MATLAB function `bvp4c` is accustomed to bolster the numerical results. The numerical results are computed by choosing different values of the involved physical parameters and compared with the earlier published results. The graphical numerical results of different physical quantities of interest are presented to analyze their dynamics under the varying physical quantities.

Contents

Author's Declaration	iv
Plagiarism Undertaking	v
Acknowledgements	vi
Abstract	vii
List of Figures	x
List of Tables	xi
Abbreviations	xii
1 Introduction	1
2 Literature review	5
2.1 Important Definition	5
2.2 Types of flow	6
2.3 Fluid properties	8
2.4 Conservation laws [39]	10
2.4.1 Conservation of mass	10
2.4.2 Conservation of momentum	11
2.4.3 Conservation of energy	11
2.5 Dimensional analysis [39]	11
2.5.1 Dimensions and units	12
2.5.2 Dimensional homogeneity	12
2.5.3 Nondimensionalization of equations	13
2.6 Dimensionless parameters	14
3 Non-uniform heat source/sink and Soret effects on MHD non-Darcian convective flow past a stretching sheet in a micropolar fluid with radiation	17
3.1 Introduction	17
3.2 Mathematical modeling	18

3.3	Dimensionless form of the model	19
3.4	Numerical Treatment	21
3.5	Results and discussion	22
4	Non-uniform heat source/sink and activation energy effects on micro polar fluid in the presence of inclined magnetic field and thermal radiation	31
4.1	Introduction	31
4.2	Problem formulation	32
4.3	Dimensionless form of the model	34
4.4	Numerical Treatment	35
4.5	Results and discussion	37
5	Conclusion	50
	Bibliography	52

List of Figures

3.1	Geometry for the flow under consideration.	18
3.2	Impact of K and M on velocity $f'(\eta)$	24
3.3	Impact of Da^{-1} and m_0 on the velocity $f'(\eta)$	25
3.4	Impact of M and K on angular velocity $g(\eta)$	25
3.5	Impact of m_0 and Da^{-1} on angular velocity $g(\eta)$	26
3.6	Impact of R and Q_0 on temperature $\theta(\eta)$	26
3.7	Impact of Q_1 and M on temperature $\theta(\eta)$	27
3.8	Impact of Ec and K on temperature $\theta(\eta)$	27
3.9	Impact of m_0 and Da^{-1} on temperature $\theta(\eta)$	28
3.10	Impact of ϵ and Pr on temperature $\theta(\eta)$	28
3.11	Impact of Gr and α on temperature $\theta(\eta)$	29
3.12	Impact of Sc and S_0 on the concentration $\phi(\eta)$	29
3.13	Impact of Gm and M on concentration $\phi(\eta)$	30
4.1	Geometry for the flow under consideration.	32
4.2	Impact of K and M on velocity $f'(\eta)$	40
4.3	Impact of Da^{-1} and m_0 on the velocity $f'(\eta)$	40
4.4	Impact of M and K on angular velocity $g(\eta)$	41
4.5	Impact of m_0 and Da^{-1} on angular velocity $g(\eta)$	41
4.6	Impact of R and Q_0 on temperature $\theta(\eta)$	42
4.7	Impact of Q_1 and M on temperature $\theta(\eta)$	42
4.8	Impact of Ec and K on temperature $\theta(\eta)$	43
4.9	Impact of m_0 and Da^{-1} on temperature $\theta(\eta)$	43
4.10	Impact of ϵ and Pr on temperature $\theta(\eta)$	44
4.11	Impact of Gr and α on temperature $\theta(\eta)$	44
4.12	Impact of Sc and S_0 on the concentration $\phi(\eta)$	45
4.13	Impact of Gm and M on concentration $\phi(\eta)$	45
4.14	Impact of σ and K on concentration $\phi(\eta)$	46
4.15	Impact of δ and M on concentration $\phi(\eta)$	46
4.16	Impact of n and M on concentration $\phi(\eta)$	47
4.17	Impact of Df and M on concentration $\phi(\eta)$	47
4.18	Impact of β and K on velocity $f'(\eta)$	48
4.19	Impact of β and K on temperature $\theta(\eta)$	48
4.20	Impact of β and n on concentration $\phi(\eta)$	49

List of Tables

3.1	Impact of different values of K on $C_f Re_x^{1/2}$ keeping all other parameters zero	22
3.2	Impact of different values of Pr on $C_f Re_x^{1/2}$ keeping all other parameters zero	22
4.1	Impact of different values of K on $C_f Re_x^{1/2}$ keeping all other parameters zero	37
4.2	Impact of different values of Pr on $C_f Re_x^{1/2}$ keeping all other parameters zero	37

Abbreviations

ODE	Ordinary differential equation
PDE	Partial differential equation
BVP	Boundary value problem
IVP	Initial value problem
MHD	Magnetohydrodynamics
BC	Boundary condition

Nomenclature

A_0, A_1 constants	T_m fluid temperature
\vec{B} transverse magnetic field	T_w wall temperature of the fluid
B_0 uniform transverse magnetic field	R thermal radiation parameter
b stretching parameter	Re_x local Reynolds number
C concentration of the species	Sc Schmidt number
C_b drag coefficient	S_0 Soret number
C_f Skin friction coefficient	Q_0 coefficient of space-dependent
C_∞ concentration of the solute far away from the sheet	heat source/sink
C_w wall concentration of the solute	Q_1 coefficient of temperature-dependent
C_p specific at constant pressure	heat source/sink
D_m mass diffusivity coefficient	q_r radiative heat flux
Da^{-1} inverse Darcy number	q_w rate of heat transfer
E_c Eckert number	q''' non uniform heat generation/absorption
f dimensionless stream function	u velocity of the fluid in the x -direction
G_m modified Grashof number	v velocity of the fluid in the y -direction
G_r Grashof number	x flow directional coordinate along the stretching sheet
g dimensionless angular velocity	y distance normal to the stretching sheet
j micro-inertia per unit mass	Greek letters
K material parameter	β inclination of magnetic field
K_T thermal diffusion ratio	β^* coefficient of concentration expansion
k_1 vortex viscosity	θ non-dimensional temperature parameter
k^* absorption coefficient	ϕ non-dimensional concentration parameter
l characteristic length	φ porosity of the porous medium
M magnetic field parameter	η similarity variable
m_0 a constant	σ electrical conductivity
m_w rate of mass transfer	ρ density of the fluid
N components of microrotation	ν kinematic viscosity
Nu_x local Nusselt number	σ^* Stefan–Boltzmann constant
T temperature of fluid	γ spin gradient viscosity

Chapter 1

Introduction

There are countless industrial applications of heat and mass transfer. The applications of mass transfer are petrochemical refining, fractional distillation, where part of crude oil is separated. In short every process of refining leverages mass transfer. Likewise, the heat transfer has a number of industrial applications e.g. in food industry meat and poultry processing, snack foods and in chemical industry for batch reactor, continuous processes and in asphalt and concrete industry for concrete heating and hot mix paving and in industrial laundry for flat work ironers and steam generators. In many other industries, the process of heat and mass transfer over a stretching sheet is being used, like glass fiber production, aerodynamic extrusion of plastic sheets, glass blowing etc. In all these applications, the obtained products quality mainly depends upon the heat transfer rate at the stretching surfaces. Many authors like Bhatti [1], Anjali and Ganga [2], Raju et al. [3] discussed the heat and mass transfer and their applications. Physically, micropolar fluids usually represent the fluids involving particles which are rigid, randomly oriented (or spherical) dangled in a viscous medium ignoring the deformation of particles. Main attention of researchers, now a days, is on the micropolar fluids because of its inclusiveness in applications such as polymeric fluids, liquid crystals and chemical suspensions. In [4–9], the micropolar fluids and its applications have been discussed. The applications of the transfer of heat and mass on MHD flow was canvassed by Mansour et al [10]. The Viscous dissipation

effects on MHD free convection flow over a nonisothermal surface in a micropolar fluid was analyzed in [11]. The effects of Joule heating and mass transfer on MHD flow of a micropolar fluid were discussed by El-hakiem et al. [12] and El-Amin [13]. Deepa and Murali [14] investigated the dissipation effects on MHD flow of a micropolar fluid.

The transfer of heat and mass subject to thermal radiation has become the most popular area of research due to its industrial applications e.g. the radiation and heat transfer plays a very important role in combustion devices due to the presence of very high temperature in combustion processes. Some other applications include, internal combustion engines, combustions of liquid propellants and in exhaust plums of liquid rockets. Abo-Eldohad and Ghonaim [15], Rahman [16] described the thermal radiation effect on the flow of micropolar fluids. Thermal radiation effects on the micropolar fluids are discussed in detail in [17–22]. Heat source/sink effects can be discussed by considering two situations. First is internal heat generation or absorption and the second is the external heat generation and absorption. Both of these are used at a very large scale in industries as well as in the laboratory experiments. It is also very important to control the heat transfer. Various studies have been conducted on heat source and sink effects including Pal and Chatterjee [23, 24], Subhas and Mahesha [25], Rahman et al. [26] and Bataler [27].

The diffusion flux occurs due to the temperature gradient named as the Soret effect. The Dufour effect which is the reciprocal of Soret effects has not been studied yet in the above studies. The Dufour effect is the energy flux which could be of any form e.g. heat energy, radiative flux and sound energy flux. To delineate the Dufour effect, a contribution of heat flux is needed which is proportional to concentration gradient. Therefore we will find its effects on the concentration distribution. Both of these effects have a vital role in the flow of gases. The Soret effect is more prominent than the Dufour effect in liquids, however the Dufour number includes in the study of liquids as well as gases, as many researchers like Khan et al. [28], Mortimer and Eyring [29], Ali et al. [30], Hayat et al. [31] has studied both effects the Soret and Dufour numbers for different flows.

The magnetic field or the magnetic surfaces play an important role in MHD. For example, along the direction of the magnetic field, the charged particles and the conducting fluid both can move easily but seldomly against it. Also, there are some functional variables on which the stability and confinement properties of fluids depend and these variables are uniform in magnetic configuration. We will see how the fluid behaves in the presence of the magnetic field at different angles. The inclined magnetic field effects on fluid flow were explored by Singh et al. [32], Seth et al. [33] and Dar [34].

Activation energy which characterizes the viscous flow, is actually a least energy required by a molecule to get out of the region where it is being influenced by the other molecules. It can also be interpreted as the amount of energy required to initiate the chemical reaction i.e for a chemical reaction to be proceed, there should be an appropriate number of molecules so that the total energy of these molecules is either equal or greater than the activation energy. Its applications involve chemical engineering, geothermal reservoirs, mechanics of water and oil emulsions, food processing etc. Researchers who evolved the activation energy's effects on different fluid flows are Monkos [35], Maleque [36], Mustafa et al. [37].

Thesis contribution:

In this work, first of all we emulate and scrutinize the work of Mabood [38]. The work of Mabood [38] is then extended by adding the effects of inclined magnetic field, activation energy and Dufour number which were not discussed yet in literature. The formulated highly non linear equations for the above mentioned flow are converted into first order ODEs under lubricant approach. The shooting method is used to solve the BVP by using the computational software MATLAB. A built-in MATLAB function `bvp4c` is accustomed to assist the numerical results. The numerical results are computed by choosing different values of the involved physical parameters and compared with the earlier published results. The graphical numerical results of different physical quantities of interest are presented to analyze

their dynamics under the varying physical quantities.

The thesis is categorized in the following order;

Chapter 2 consists of some basic definitions and terminologies which are very helpful in understanding the whole work.

Chapter 3 emulates and scrutinizes the work of Mabood [38]. The whole work in this chapter is reproduced by using the shooting method. A built-in MATLAB function `bvp4c` is accustomed to assist the numerical results.

Chapter 4 extends the idea of Mabood [38] by including Dufour number, activation energy and magnetic field.

Chapter 5 consists of the conclusions derived from the entire work .

References which are used in this dissertation are catalogued in **Bibliography**.

Chapter 2

Literature review

In the current chapter, some definitions, basic laws, terminologies, would be described which would be used in next chapters.

2.1 Important Definition

Definition 2.1.1 (Fluid). [39]

“You will recall from physics that a substance exists in three primary phases: solid, liquid, and gas. (At very high temperatures, it also exists as plasma.) A substance in the liquid or gas phase is referred to as a fluid. Distinction between a solid and a fluid is made on the basis of the substances ability to resist an applied shear (or tangential) stress that tends to change its shape. A solid can resist an applied shear stress by deforming, whereas a fluid deforms continuously under the influence of shear stress, no matter how small. In solids stress is proportional to strain, but in fluids stress is proportional to strain rate. When a constant shear force is applied, a solid eventually stops deforming, at some fixed strain angle, whereas a fluid never stops deforming and approaches a certain rate of strain.”

Definition 2.1.2 (Fluid mechanics). [39]

“Fluid mechanics is defined as the science that deals with the behavior of fluids at

rest (fluid statics) or in motion (fluid dynamics) and the interaction of fluids with solid or other fluids at the boundaries.”

Definition 2.1.3 (Fluid dynamics). [40]

“It is the study of the motion of liquids, gases and plasmas from one place to another. Fluid dynamics has a wide range of applications like calculating force and moments on aircraft, mass flow rate of petroleum passing through pipelines, prediction of weather, etc.”

Definition 2.1.4 (Hydrodynamics). [39]

“The study of the motion of fluids that are practically incompressible such as liquids, especially water and gases at low speeds is usually referred to as hydrodynamics.”

Definition 2.1.5 (Magnetohydrodynamics). [41]

“Magnetohydrodynamics (MHD) is concerned with the flow of electrically conducting fluids in the presence of magnetic fields, either externally applied or generated within the fluid by inductive action.”

Definition 2.1.6 (Micropolar fluid). [40]

“Micropolar fluids are fluids with microstructures. Physically, the micropolar fluids may represent fluids consisting of rigid, randomly oriented(or spherical) particles suspended in a viscous medium, where the deformation of the fluid particles is ignored.”

2.2 Types of flow

Definition 2.2.1 (Compressible and incompressible flows). [39]

“A flow is classified as being compressible or incompressible, depending on the level of variation of density during flow. Incompressibility is an approximation, and a flow is said to be incompressible if the density remains nearly constant throughout. Therefore, the volume of every portion of fluid remains unchanged over the course of its motion when the flow (or the fluid) is incompressible. The densities of liquids

are essentially constant, and thus the flow of liquids is typically incompressible. Therefore, liquids are usually referred to as incompressible substances. A pressure of 210 atm, for example, causes the density of liquid water at 1 atm to change by just 1 percent. Gases, on the other hand, are highly compressible. A pressure change of just 0.01 atm, for example, causes a change of 1 percent in the density of atmospheric air.”

Definition 2.2.2 (Steady versus unsteady flow). [39]

“The terms steady and uniform are used frequently in engineering, and thus it is important to have a clear understanding of their meanings. The term steady implies no change at a point with time. The opposite of steady is unsteady. The term uniform implies no change with location over a specified region. These meanings are consistent with their everyday use (steady girlfriend, uniform distribution, etc.). The terms unsteady and transient are often used interchangeably, but these terms are not synonyms. In fluid mechanics, unsteady is the most general term that applies to any flow that is not steady, but transient is typically used for developing flows. When a rocket engine is fired up, for example, there are transient effects (the pressure builds up inside the rocket engine, the flow accelerates, etc.) until the engine settles down and operates steadily. The term periodic refers to the kind of unsteady flow in which the flow oscillates about a steady mean.”

Definition 2.2.3 (Laminar versus turbulent flow). [39]

“Some flows are smooth and orderly while others are rather chaotic. The highly ordered fluid motion characterized by smooth layers of fluid is called laminar. The word laminar comes from the movement of adjacent fluid particles together in laminates. The flow of high-viscosity fluids such as oils at low velocities is typically laminar. The highly disordered fluid motion that typically occurs at high velocities and is characterized by velocity fluctuations is called turbulent. The flow of low-viscosity fluids such as air at high velocities is typically turbulent. The flow regime greatly influences the required power for pumping. A flow that alternates between being laminar and turbulent is called transitional.”

Definition 2.2.4 (Viscous and inviscid flow). [39]

“When two fluid layers move relative to each other, a friction force develops between them and the slower layer tries to slow down the faster layer. This internal resistance to flow is quantified by the fluid property viscosity, which is a measure of internal stickiness of the fluid. Viscosity is caused by cohesive forces between the molecules in liquids and by molecular collisions in gases. There is no fluid with zero viscosity, and thus all fluid flows involve viscous effects to some degree. Flows in which the frictional effects are significant are called viscous flows. However, in many flows of practical interest, there are regions (typically regions not close to solid surfaces) where viscous forces are negligibly small compared to inertial or pressure forces. Neglecting the viscous terms in such inviscid flow regions greatly simplifies the analysis without much loss in accuracy.”

Definition 2.2.5 (Newtonian and non-Newtonian fluids). [42]

“Fluids for which the viscosity is not independent of the rate of shear are referred as non-Newtonian and the liquids for which the viscosity is independent of the rate of shear are called Newtonian fluids.”

2.3 Fluid properties

Definition 2.3.1 (Heat transfer). [43]

“The study of heat transfer is directed to

1-The estimation of rate of flow of energy as heat through the boundary of the system both under steady and transient conditions

2-The determination of temperature field under steady and transient conditions, which also will provide the information about the gradient and time rate of change of temperature at various locations and time. ”

Definition 2.3.2 (Mass Transfer). [43]

“Mass transfer is the flow of molecules from one body to another when these bodies are in contact or within a system consisting of two components when the distribution of materials is not uniform. When a copper plate is placed on a steel

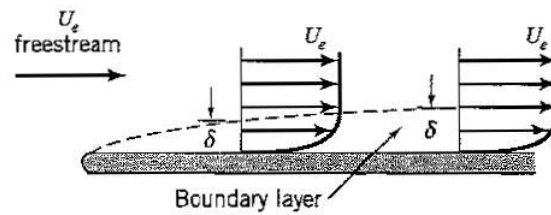
plate, some molecules from either side will diffuse into the other side. When salt is placed in a glass and water poured over it, after sufficient time the salt molecules will diffuse into the water body. A more common example is drying of clothes or the evaporation of water spilled on the floor when water molecules diffuse into the air surrounding it. Usually mass transfer takes place from a location where the particular component is proportionately high to a location where the component is proportionately low. Mass transfer may also take place due to potentials other than concentration difference.”

Definition 2.3.3 (Thermal radiation). [43]

“The process by which heat is transferred from a body by virtue of its temperature, without the aid of any intervening medium, is called thermal radiation. Sometimes radiant energy is taken to be transported by electromagnetic waves while at other times it is supposed to be transported by particle like photons. Radiation is found to travel at the speed of light in vacuum. The term Electromagnetic radiation encompasses many types of radiation namely short wave radiation like gamma ray, x-ray, microwave, and long wave radiation like radio wave and thermal radiation. The cause for the emission of each type of radiation is different. Thermal radiation is emitted by a medium due to its temperature.”

Definition 2.3.4 (Boundary layer). [44]

“Viscous effects are particularly important near the solid surfaces, where the strong interaction of the molecules of the fluid with molecules of the solid causes the relative velocity between the fluid and the solid to become almost exactly zero for a stationary surface. Therefore, the fluid velocity in the region near the wall must reduce to zero. This is called no slip condition. In that condition there is no relative motion between the fluid and the solid surface at their point of contact. It follows that the flow velocity varies with distance from the wall; from zero at the wall to its full value some distance away, so that significant velocity gradients are established close to the wall. In most cases this region is thin (compared to the typical body dimension), and it is called a boundary layer. ”



2.4 Conservation laws [39]

“You are already familiar with numerous conservation laws such as the laws of conservation of mass, conservation of energy, and conservation of momentum. Historically, the conservation laws are first applied to a fixed quantity of matter called a closed system or just a system, and then extended to regions in space called control volumes. The conservation relations are also called balance equations since any conserved quantity must balance during a process. We now give a brief description of the conservation of mass, momentum, and energy relations.”

2.4.1 Conservation of mass

“The conservation of mass relation for a closed system undergoing a change is expressed as $m_{sys} = \text{constant}$ or $dm_{sys}/dt = 0$, which is a statement of the obvious that the mass of the system remains constant during a process. For a control volume (CV), mass balance is expressed in the rate form as

$$m_{in} - m_{out} = \frac{dm_{CV}}{dt}$$

where m_{in} and m_{out} are the total rates of mass flow into and out of the control volume, respectively, and dm_{CV}/dt is the rate of change of mass within the control volume boundaries. In fluid mechanics, the conservation of mass relation written for a differential control volume is usually called the continuity equation.”

2.4.2 Conservation of momentum

“The product of the mass and the velocity of a body is called the linear momentum or just the momentum of the body, and the momentum of a rigid body of mass m moving with a velocity \vec{V} is $m\vec{V}$. Newtons second law states that the acceleration of a body is proportional to the net force acting on it and is inversely proportional to its mass, and that the rate of change of the momentum of a body is equal to the net force acting on the body. Therefore, the momentum of a system remains constant when the net force acting on it is zero, and thus the momentum of such systems is conserved. This is known as the conservation of momentum principle.”

2.4.3 Conservation of energy

“Energy can be transferred to or from a closed system by heat or work, and the conservation of energy principle requires that the net energy transfer to or from a system during a process be equal to the change in energy content of the system. Control volumes involve energy transfer via mass flow also, and the conservation of energy principle, also called the energy balance, is expressed as.

$$E_{in} - E_{out} = \frac{dE_{cv}}{dt}$$

where E_{in} and E_{out} are the total rates of energy transfer into and out of the control volume, respectively, and dE_{CV}/dt is the rate of change of energy within the control volume boundaries. In fluid mechanics, we usually limit our consideration to mechanical forms of energy only.”

2.5 Dimensional analysis [39]

“The dimensional analysis is a powerful tool for engineers and scientists in which the combination of dimensional variables, nondimensional variables, and dimensional constants into nondimensional parameters reduces the number of necessary

independent parameters in a problem.”

2.5.1 Dimensions and units

“A dimension is the measure of a physical quantity (without numerical values), while a unit is a way to assign a number to that dimension. For example, length is a dimension that is measured in units such as microns (μm), feet (ft), centimeters (cm), meters (m), kilometers (km), etc. Further, force has the same dimensions as mass times acceleration (by Newtons’s second law). Thus, in terms of primary dimensions, dimensions of force:

$$\text{Force} = \frac{\text{Mass length}}{\text{time}^2} = \frac{mL}{t^2},$$

”

2.5.2 Dimensional homogeneity

“Weve all heard the old saying, You cant add apples and oranges. This is actually a simplified expression of a far more global and fundamental mathematical law for equations, the law of dimensional homogeneity, stated as

Every additive term in an equation must have the same dimensions.

Consider, for example, the change in total energy of a simple compressible closed system from one state and/or time(1) to another (2). The change in total energy of the system E is given by

$$\Delta E = \Delta U + \Delta KE + \Delta PE. \tag{2.1}$$

where E has three components: internal energy (U), kinetic energy (KE), and potential energy (PE). These components can be written in terms of the system mass (m); measurable quantities and thermodynamic properties at each of the two states, such as speed (V), elevation (z), and specific internal energy (u); and the known gravitational acceleration constant (g),

$\Delta U = m(u_2 - u_1)$, $\Delta KE = \frac{1}{2}m(V_2^2 - V_1^2)$, $\Delta PE = mg(Z_2 - Z_1)$. It is straightforward to verify that the left side of Eq. (2.1) and all three additive terms on the right side of above equations have the same dimensionsenergy. Using the definitions of above equations, we write the primary dimensions of each term, $\{\Delta E\} = \{\text{Energy}\} = \{\text{Force.Length}\} \rightarrow \{\Delta E\} = \left\{\frac{mL^2}{t^2}\right\}$

$$\{\Delta U\} = \left\{\text{Mass}\frac{\text{Energy}}{\text{Mass}}\right\} = \{\text{Energy}\} \rightarrow \{\Delta U\} = \left\{\frac{mL^2}{t^2}\right\}$$

$$\{\Delta KE\} = \left\{\text{Mass}\frac{\text{Length}^2}{\text{time}^2}\right\} \rightarrow \{\Delta KE\} = \left\{\frac{mL^2}{t^2}\right\}$$

$$\{\Delta PE\} = \left\{\text{Mass}\frac{\text{Length}}{\text{time}^2}\text{Length}\right\} \rightarrow \{\Delta PE\} = \left\{\frac{mL^2}{t^2}\right\}.$$

If at some stage of an analysis we find ourselves in a position in which two additive terms in an equation have different dimensions, this would be a clear indication that we have made an error at some earlier stage in the analysis. In addition to dimensional homogeneity, calculations are valid only when the units are also homogeneous in each additive term. For example, units of energy in the above terms may be J , N , m , or kg , m_2/s_2 , all of which are equivalent. Suppose, however, that kJ were used in place of J for one of the terms. This term would be off by a factor of 1000 compared to the other terms. It is wise to write out all units when performing mathematical calculations in order to avoid such errors.”

2.5.3 Nondimensionalization of equations

“The law of dimensional homogeneity guarantees that every additive term in an equation has the same dimensions. It follows that if we divide each term in the equation by a collection of variables and constants whose product has those same dimensions, the equation is rendered nondimensional. If, in addition, the nondimensional terms in the equation are of order unity, the equation is called normalized. Normalization is, thus, more restrictive than nondimensionalization, even though the two terms are sometimes (incorrectly) used interchangeably. Each term

in nondimensional equation is dimensionless. In the process of nondimensionalizing of an equation of motion, nondimensional parameters often appear—most of which are named after a notable scientist or engineer (e.g., the Reynolds number and the Froude number). This process is referred to by some authors as the inspectional analysis.”

2.6 Dimensionless parameters

Definition 2.6.1 (Skin friction coefficient). [45]

“It is a dimensionless number and is defined as

$$C_f = \frac{\tau_w}{2\rho w_\infty^2},$$

where τ_w is the local wall shear stress, ρ is the fluid density and w_∞ is the free stream velocity (usually taken outside of the boundary layer or at the inlet). It expresses the dynamic friction resistance originating in viscous fluid flow around a fixed wall.”

Definition 2.6.2 (Eckert number). [45]

“The Eckert number (Ec) is a dimensionless number used in the continuum mechanics. It expresses the relationship between a flow’s kinetic energy and enthalpy, and is used to characterize the dissipation. It is defined as

$$Ec = \frac{w_\infty^2}{C_p \Delta T},$$

where w_∞ (ms^{-1}) fluid flow velocity far from body, C_p is the constant pressure local specific heat of continuum, ΔT is temperature difference. It expresses the ratio of kinetic energy to a thermal energy change.”

Definition 2.6.3 (Prandtl number). [45]

“The Prandtl number which is a dimensionless number, named after the German

physicist Ludwig Prandtl, is defined as

$$Pr = \frac{\nu}{\alpha} \implies \frac{\mu/\rho}{k/c_p} \implies \frac{\eta c_p}{\lambda},$$

where η stands for the dynamic viscosity, C_p denotes the specific heat and λ represents the thermal conductivity. This number expresses the ratio of the momentum diffusivity (viscosity) to the thermal diffusivity. It characterizes the physical properties of a fluid with convective and diffusive heat transfers. It describes, for example, the phenomena connected with the energy transfer in a boundary layer. It expresses the degree of similarity between velocity and diffusive thermal fields or, alternatively, between hydrodynamic and thermal boundary layers.”

Definition 2.6.4 (Schmidt number). [45]

“

$$Sc = \frac{\mu}{\rho D_m} = \frac{\nu}{D_m},$$

where ν is the kinematic viscosity. D_m is mass diffusivity. μ is the dynamic viscosity of the fluid. ρ is the density of the fluid. This number expresses the ratio of the kinematic viscosity, or momentum transfer by internal friction, to the molecular diffusivity. It characterizes the relation between the material and momentum transfers in mass transfer. It provides the similarity of velocity and concentration fields in mass transfer. For example, molten materials with an equal Schmidt number have similar velocity and concentration fields. Higher Sc number values characterize slower mass exchange and higher values of dividing coefficients. This leads to higher mixing and a tendency to crack in a solidified casting. The criterion was first introduced by Schmidt in 1929.”

Definition 2.6.5 (Grashof number). [45]

“

$$Gr = L^3 g \frac{\beta_T(\Delta T)}{\nu^2}, \text{ for temperature profile}$$

L - characteristic length dimension, g -gravitational acceleration, ΔT -temperature change, β -volume thermal expansion coefficient. It expresses the buoyancy-to-viscous forces ratio and its action on a fluid. It characterizes the free non-isothermal convection of the fluid due to the density difference caused by the

temperature gradient in the fluid.”

Chapter 3

Non-uniform heat source/sink and Soret effects on MHD non-Darcian convective flow past a stretching sheet in a micropolar fluid with radiation

3.1 Introduction

In the present chapter the effects of Soret number, variable thermal conductivity, viscous-Ohmic dissipation on the two-dimensional hydromagnetic mixed convective heat and mass transfer flow of a micropolar fluid over a stretching sheet embedded in a non-Darcian porous medium with thermal radiation, have been discussed. The formulated highly non linear equations for the above mentioned flow are converted into first order ODEs. The shooting method is used to solve the BVP by using the computational software MATLAB. A built-in MATLAB function `bvp4c` is accustomed to assist the numerical results. The numerical results are computed by choosing different values of the involved physical parameters and

compared with the earlier published results. The behaviour of velocity, angular velocity, temperature and concentration, for different physical parameters has been investigated. The graphs and tables which are obtained under this investigation are given and analyzed at the end of this chapter.

3.2 Mathematical modeling

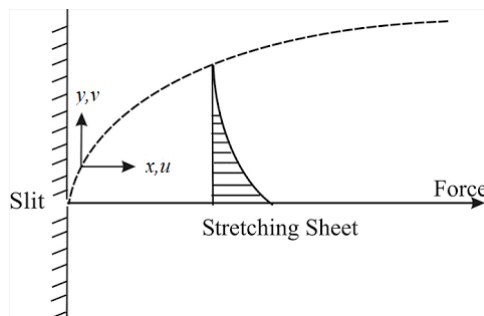


FIGURE 3.1: Geometry for the flow under consideration.

A 2-D steady mixed convection flow of an incompressible, electrically conducting micropolar fluid has been considered. The fluid is assumed to flow above and along x -axis such that y -axis is perpendicular to the fluid motion. Two equal and opposite forces are brought into action by stretching the sheet to generate the flow. The sheet is stretched so that the velocity at each instant is proportional to the distance from its origin ($x = 0$). The fluid is flowing under the influence of the magnetic field. The frictional and Ohmic heating are also considered in flow, produced by the viscous dissipation and Soret effects respectively. The equations of considered basic laws for flow are given below:

$$\frac{\partial u}{\partial x} + \frac{\partial v}{\partial y} = 0, \quad (3.1)$$

$$u \frac{\partial u}{\partial x} + v \frac{\partial u}{\partial y} = \left(\nu + \frac{k_1}{\rho} \right) \frac{\partial^2 u}{\partial y^2} + \frac{k_1}{\rho} \frac{\partial N}{\partial y} - \frac{\nu \varphi}{k} u - \frac{C_b \varphi}{\sqrt{k}} u^2 - \frac{\sigma B_0^2}{\rho} u + g\beta'(T - T_\infty) + g\beta^*(C - C_\infty), \quad (3.2)$$

$$\rho j \left(u \frac{\partial N}{\partial x} + v \frac{\partial N}{\partial y} \right) = \gamma \frac{\partial^2 N}{\partial y^2} - k_1 \left(2N + \frac{\partial u}{\partial y} \right). \quad (3.3)$$

$$u \frac{\partial T}{\partial x} + v \frac{\partial T}{\partial y} = \frac{1}{\rho C_p} \frac{\partial}{\partial y} \left(K \frac{\partial T}{\partial y} \right) - \frac{1}{\rho C_p} \frac{\partial q_r}{\partial y} + \frac{\sigma B_0^2}{\rho C_p} u^2 + \frac{q'''}{\rho C_p} + \frac{\mu}{\rho C_p} \left(\frac{\partial u}{\partial y} \right)^2, \quad (3.4)$$

$$u \frac{\partial C}{\partial x} + v \frac{\partial C}{\partial y} = D_m \frac{\partial^2 C}{\partial y^2} + \frac{D_m k_T}{T_m} \frac{\partial^2 T}{\partial y^2}. \quad (3.5)$$

The associated boundary conditions are:

$$\left. \begin{aligned} u = u_w = bx, \quad v = 0, \quad N = -m \frac{\partial u}{\partial y}, \quad T = T_w = T + A_0 \left(\frac{x}{l} \right)^2, \\ C = C_w = C + A_1 \left(\frac{x}{l} \right)^2 \quad \text{at } y = 0, \\ u \rightarrow 0, \quad N \rightarrow 0, \quad T \rightarrow T_\infty, \quad C \rightarrow C_\infty \quad \text{as } y \rightarrow \infty. \end{aligned} \right\} \quad (3.6)$$

where u and v are the horizontal and vertical components of velocities.

3.3 Dimensionless form of the model

To solve the above system of PDEs numerically, we first convert it into the non-dimensionalized form. For this we use the following dimensionless variables:

$$\left. \begin{aligned} \eta = \sqrt{\frac{b}{\nu}} y, \quad N = bx \sqrt{\frac{b}{\nu}} g(\eta), \quad u = bx f'(\eta), \quad v = \sqrt{b\nu} f(\eta), \quad \theta(\eta) = \frac{T - T_\infty}{T_w - T_\infty}, \\ \phi(\eta) = \frac{C - C_\infty}{C_w - C_\infty}, \\ T - T_\infty = A_0 \left(\frac{x}{l} \right)^2 \theta(\eta), \quad T_w - T_\infty = A_0 \left(\frac{x}{l} \right)^2, \quad C - C_\infty = A_1 \left(\frac{x}{l} \right)^2 \phi(\eta), \\ C_w - C_\infty = A_1 \left(\frac{x}{l} \right)^2. \end{aligned} \right\} \quad (3.7)$$

where f and g are the stream and microrotation functions respectively and both are dimensionless, η is the similarity variable, l is the characteristic length. The above, equation (3.1) is satisfied identically. Remaining governing Eqs are transformed into the following form:

$$(1 + K)f''' + ff'' - (f')^2 - Da^{-1}f' - \alpha(f')^2 + kg' - Mf' + Gr\theta + Gm\phi = 0, \quad (3.8)$$

$$\left(1 + \frac{K}{2}\right)g'' - K(2g + f'') - f'g + fg' = 0, \quad (3.9)$$

$$(1 + R + \epsilon\theta)\theta'' + Pr(f\theta' - 2f'\theta) + \epsilon(\theta')^2 + PrMEc(f')^2 + PrEc(f'')^2 \quad (3.10)$$

$$+ (1 + \epsilon\theta)(Q_0f' + Q_1\theta) = 0, \quad (3.11)$$

$$\phi'' + Sc(\phi'f - 2\phi f') + ScS_0\theta'' = 0. \quad (3.12)$$

The BCs, now, become:

$$f(\eta) = 0, \quad f'(\eta) = 1, \quad g(\eta) = -m_0f''(\eta), \quad \theta(\eta) = 1, \quad \phi(\eta) = 1 \text{ at } \eta = 0, \quad (3.13)$$

$$f'(\eta) \rightarrow 0, \quad g(\eta) \rightarrow 0, \quad \theta(\eta) \rightarrow 0, \quad \phi(\eta) \rightarrow 0, \text{ as } \eta \rightarrow \infty. \quad (3.14)$$

The dimensionless parameters are defined as

$$\left. \begin{aligned} Da^{-1} &= \frac{\phi\nu}{kb}, \quad M = \frac{\sigma}{\rho b}B_0^2, \quad Gr = \frac{g\beta'(T - T_\infty)}{b^2l}, \quad G_m = \frac{g\beta^*(C - C_\infty)}{b^2l}, \quad K = \frac{k_1}{\mu}, \\ E_c &= \frac{b^2l}{A_0C_p}, \quad R = \frac{16T_\infty^3\sigma^*}{3k^*k_\infty}, \quad Sc = \frac{\nu}{D_m}, \quad S_0 = \frac{k_T(T_w - T_\infty)}{T_m(C_w - C_\infty)}, \quad Pr = \frac{\mu C_p}{K_\infty}. \end{aligned} \right\} \quad (3.15)$$

The skin-friction coefficient C_f , Nusselt number Nu_x and Sherwood number Sh_x are defined as

$$C_f = \frac{\tau_w}{\rho u_w^2}, \quad Nu_x = \frac{xq_w}{k(T_w - T_\infty)}, \quad Sh_x = \frac{xm_w}{D_m(C_w - C_\infty)}. \quad (3.16)$$

Here, the heat flux q_w , the skin-friction on flat plate τ_w , and the mass transfer rate m_w are given by

$$\tau_w = \left(|\mu + k_1| \frac{\partial u}{\partial y}\right)_{y=0}, \quad q_w = -K \left(\frac{\partial T}{\partial y}\right)_{y=0}, \quad m_w = -D_m \left(\frac{\partial C}{\partial y}\right)_{y=0}. \quad (3.17)$$

By using the above equations, we have

$$C_f Re_x^{1/2} = (1 + K)f'(0), \quad Nu_x = -\sqrt{Re_x}\theta(0), \quad Sh_x = -\sqrt{Re_x}\phi(0). \quad (3.18)$$

Here, $Re_x = \frac{u_w x}{\nu}$ is the local Reynolds number.

3.4 Numerical Treatment

This section is focused on the implementation of the shooting method to solve the transformed ODEs (3.8)-(3.11) subject to the boundary conditions (3.12)-(3.13). For this purpose, we first convert the system of ODEs into first order ODEs, by using the following notations

$$f = y_1, f' = y_2, f'' = y_3, g = y_4, g' = y_5, \theta = y_6, \theta' = y_7, \phi = y_8, \phi' = y_9. \quad (3.19)$$

The resulting system of first order ODEs is:

$$\begin{aligned} y_1' &= y_2, \\ y_2' &= y_3, \\ y_3' &= \left(\frac{1}{1+K} \right) (-y_1 y_3 + y_2^2 + Da^{-1} y_2 + \alpha y_2^2 - k y_5 + M y_2 - G r y_6 - G m y_8), \\ y_4' &= y_5, \\ y_5' &= \frac{2}{2+K} (K(2y_4 + y_3) + y_2 y_4 - y_1 y_5), \\ y_6' &= y_7, \\ y_7' &= \frac{1}{(1+R+\epsilon y_6)} (-y_1 y_7 - 2y_2 y_6) - \epsilon y_7^2 - PrMEcy_2^2 - PrEcy_3^2 \\ &\quad - (1+\epsilon y_6)(Q_0 y_2 + Q_1 y_6), \\ y_8' &= y_9, \\ y_9' &= -Sc(y_9 y_1 - 2y_8 y_2 + S_0 y_7'). \end{aligned}$$

The resulting form of the BCs is

$$\begin{aligned} y_1(0) &= 0, y_2(0) = 1, y_4(0) = -m_0 y_3(0), y_6(0) = 1, y_8(0) = 1, \\ y_2 &\rightarrow 0, y_4 \rightarrow 0, y_6 \rightarrow 0, y_8 \rightarrow 0 \text{ as } \eta \rightarrow \infty. \end{aligned}$$

TABLE 3.1: Impact of different values of K on $C_f Re_x^{1/2}$ keeping all other parameters zero

K	[46]	[38]	Current Results
0	-1.000000	-1.000008	-1.0000083
1	-1.367872	-1.367996	-1.3679962
2	-1.621225	-1.621575	-1.6215750
3	-	-1.827382	-1.8273821
4	-2.004133	-2.005420	-2.0054202
5	-	-2.164823	-2.1648229

TABLE 3.2: Impact of different values of Pr on $C_f Re_x^{1/2}$ keeping all other parameters zero

Pr	[47]	[48]	[19]	[23]	[38]	Current Results
1	1.3333	1.33334	1.3333	1.333333	1.33333334	1.33333334
3	2.5097	2.50997	2.5097	2.509725	2.50972157	2.50972157
10	4.7969	4.79686	4.7969	4.796873	4.79687059	4.79687058

To solve these equations numerically, the unbounded domain $[0, \infty)$ is replaced by an appropriate domain $[0, \eta_{max}]$. To solve the above ODEs by the shooting method, the initial values of $y_3(0)$, $y_5(0)$, $y_7(0)$, $y_9(0)$ are chosen arbitrarily. During the execution of iterations these initial guesses will be updated by the Newton's method and the process will be continued until the following criteria is met

$$\max\{|y_2(\eta_{max}) - 0|, |y_4(\eta_{max}) - 0|, |y_6(\eta_{max}) - 0|, |y_8(\eta_{max}) - 0|\} < \xi$$

Throughout this work, ξ has been taken as $(10)^{-5}$ unless otherwise mentioned

3.5 Results and discussion

For the validity of our MATLAB code, the skin friction factor and the local Nusselt number have been compared with those already published in literature as shown in Tables 3.1 and 3.2.

From tables it can be seen that the results achieved by the present code are found convincingly very closed to the published results.

Fig. 3.2 represents the velocity profile for different values of K and M while all other parameters are kept constant. We can see from this figure that as the value of M is escalated the velocity profile declined and a reverse scenario is observed in the case of material parameter K . The velocity is decreased by increasing the values of M because of an opposite force named as the Lorentz force, which has the tendency to reduce the velocity. Figure 3.3 divulges the velocity profile for changing values of Da^{-1} and m_0 while all other parameters are kept constant. Figure shows that the velocity profile gets sharper for increasing value of Da^{-1} and m_0 . In Figure, 3.4 it can be seen that as we increase the values of K and M , the angular velocity increases while all other parameters have the fixed values. Figure 3.5 divulges that as we increase the values of Da^{-1} and m_0 , the angular velocity increases near the wall while all other parameters have fixed values. Figure 3.6 delineates the effect of Q_0 and R on the dimensionless temperature profile $\theta(\eta)$. It is found that with the increasing values of Q_0 and R , the thermal boundary layer thickness increases. An increment in Q_0 allows the flow to become more energetic, this increment in energy increases the overall temperature of the fluid. Figure 3.7 depicts the behaviour of the dimensionless temperature $\theta(\eta)$ which escalates with escalation of M and declines with the declination of Q_1 . As we increase M , the opposite Lorentz force comes into act which offers resistance to the flow and thus the thermal boundary layer thickness is increased. Figure 3.8 depicts the behaviour of the dimensionless temperature $\theta(\eta)$ which is observed to increase with an augmentation in the Ec and decrease for increasing values of K . The physical reason behind it is that an increment in the dissipation enhances the thermal conductivity of the fluid which causes an enhancement in the thermal boundary layer. It is clear from Figure 3.9 that if we increase the inverse Darcy number and constant number m_0 the value of $\theta(\eta)$ increases. In Figure 3.10 it has been illustrated that the temperature profile increases as the physical parameter ϵ increases and decreases with an increment in Pr . This is because when we increase the Prandtl number Pr , heat diffuses casually away from the sheet, as a result

the temperature and the thermal boundary layer thickness reduce. Figure 3.11 demonstrates the influence of Grashof number Gr and local inertia-coefficient α on temperature profile. Here $\theta(\eta)$ is direct in proportion with α and inverse in proportion with Gr . Figure 3.12 is the illustration of dimensionless concentration with varying values of S_0 and Sc . We can see that $\phi(\eta)$ escalate as S_0 escalate and decline as Sc escalate. Physically Sc is the ratio of momentum to mass diffusivities, so for larger Sc mass diffusivity reduces which causes decadence in ϕ . Figure 3.13 is the illustration of dimensionless concentration with varying values of Gm and M . We can see that $\phi(\eta)$ escalate as M escalate and decline as Gm escalate.

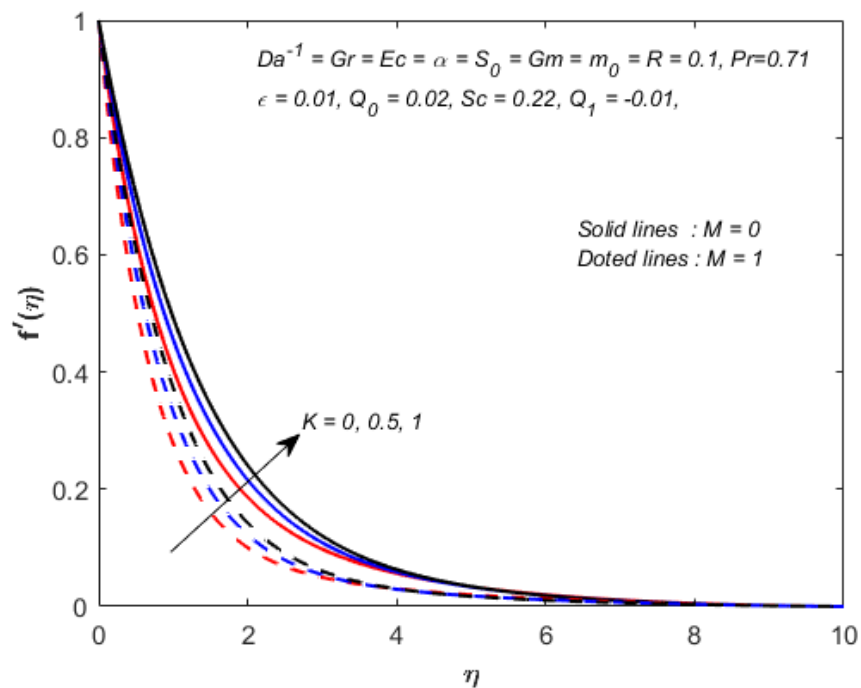


FIGURE 3.2: Impact of K and M on velocity $f'(\eta)$

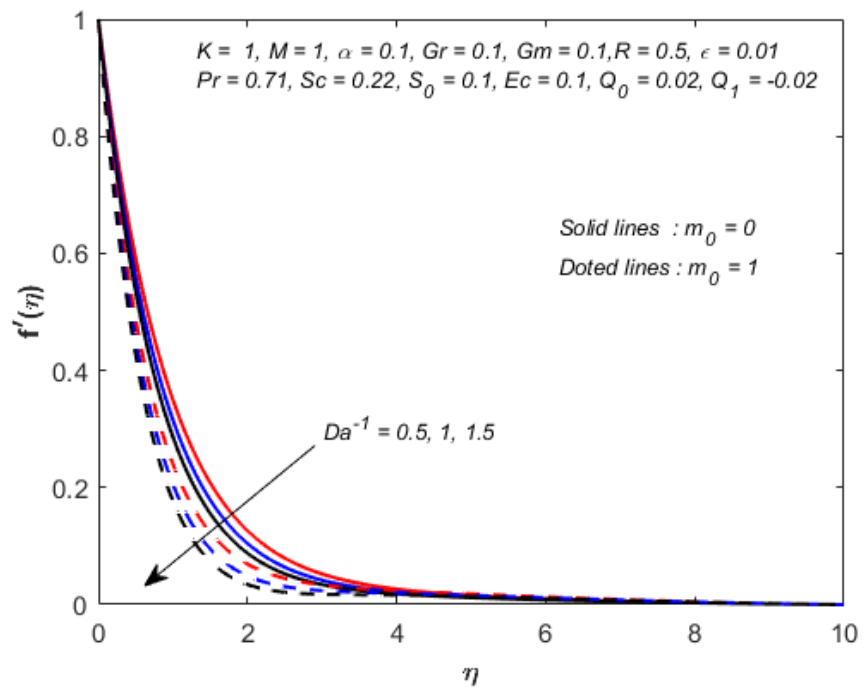


FIGURE 3.3: Impact of Da^{-1} and m_0 on the velocity $f'(\eta)$

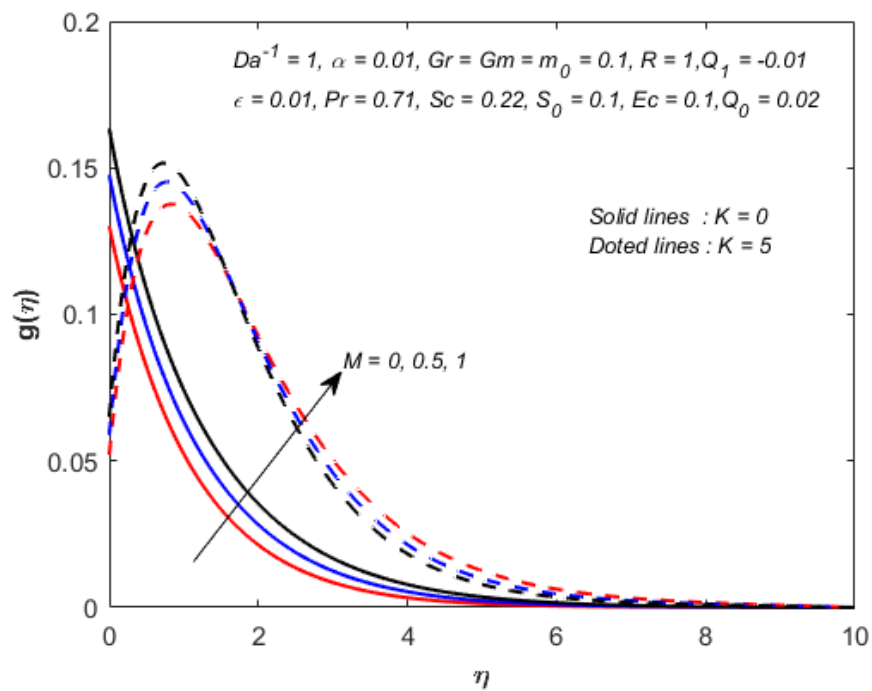


FIGURE 3.4: Impact of M and K on angular velocity $g(\eta)$

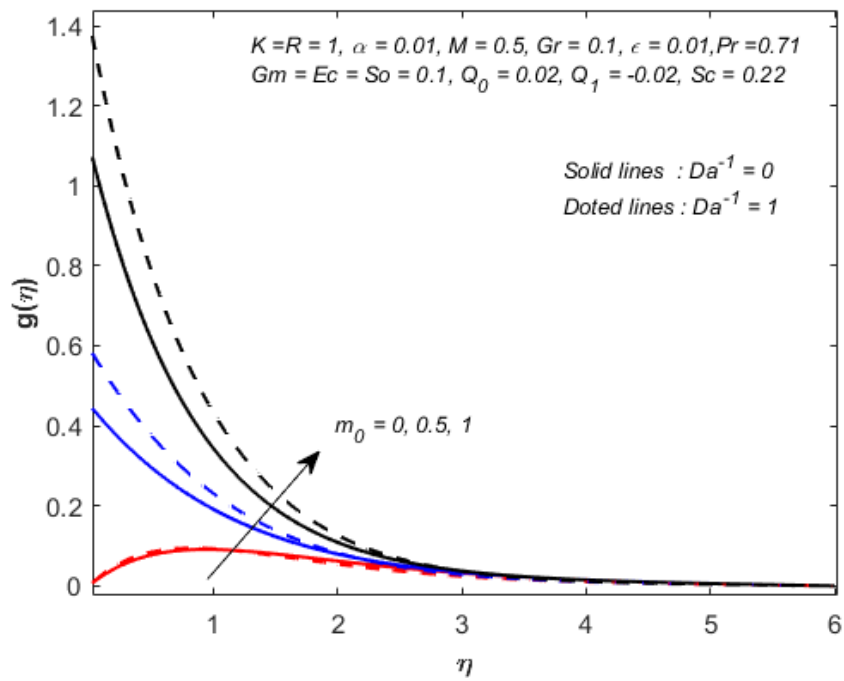


FIGURE 3.5: Impact of m_0 and Da^{-1} on angular velocity $g(\eta)$

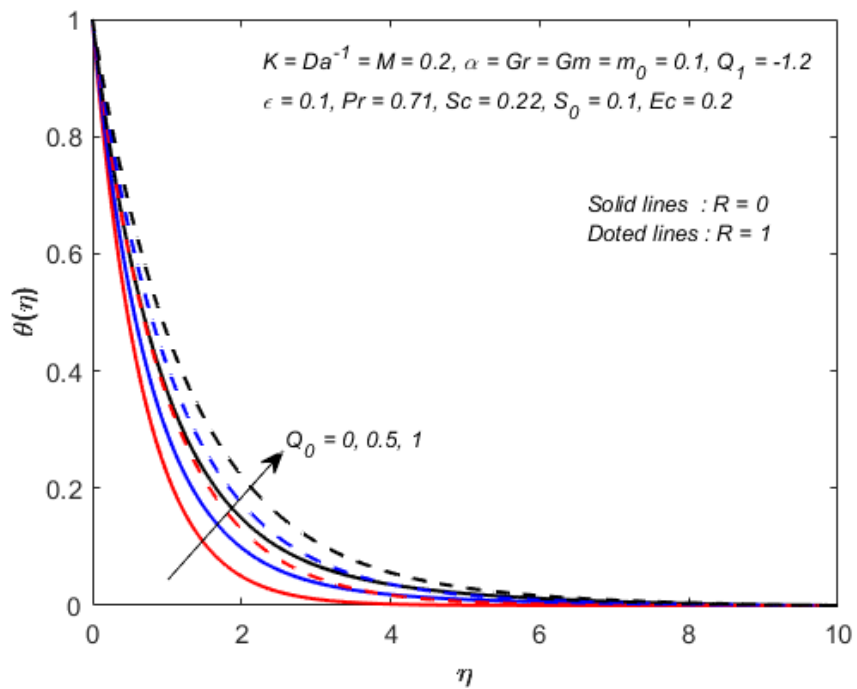


FIGURE 3.6: Impact of R and Q_0 on temperature $\theta(\eta)$

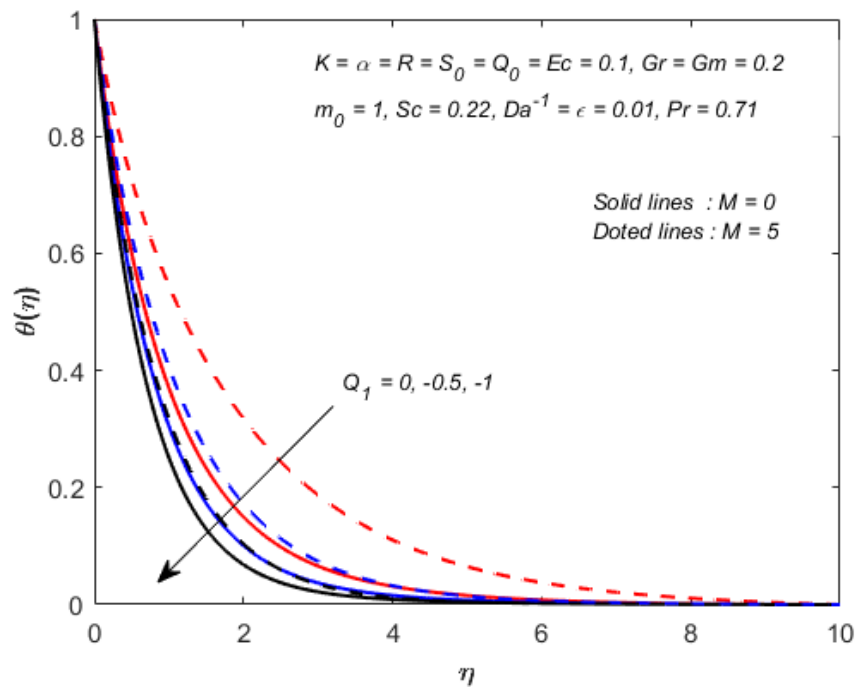


FIGURE 3.7: Impact of Q_1 and M on temperature $\theta(\eta)$

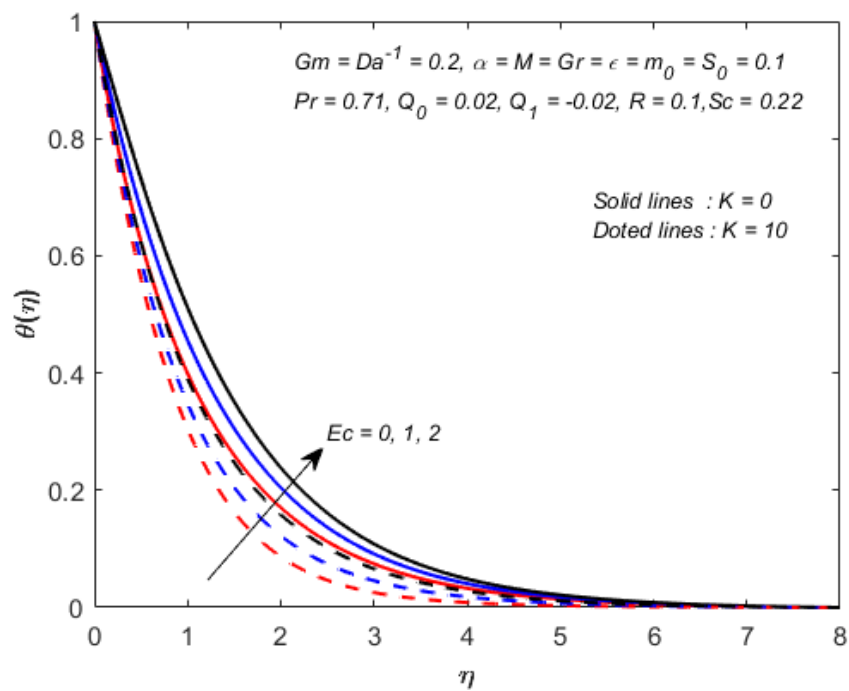


FIGURE 3.8: Impact of Ec and K on temperature $\theta(\eta)$

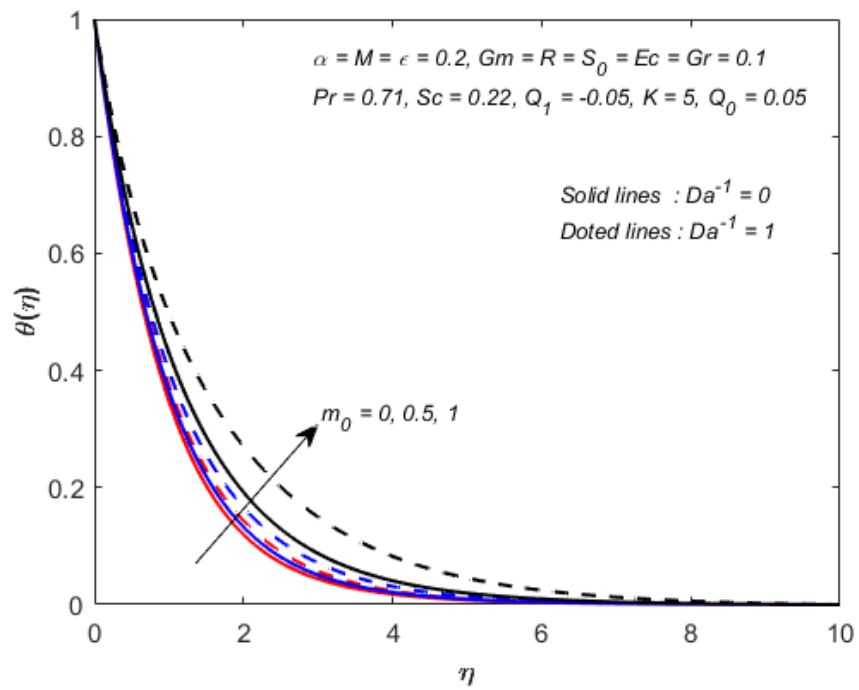


FIGURE 3.9: Impact of m_0 and Da^{-1} on temperature $\theta(\eta)$

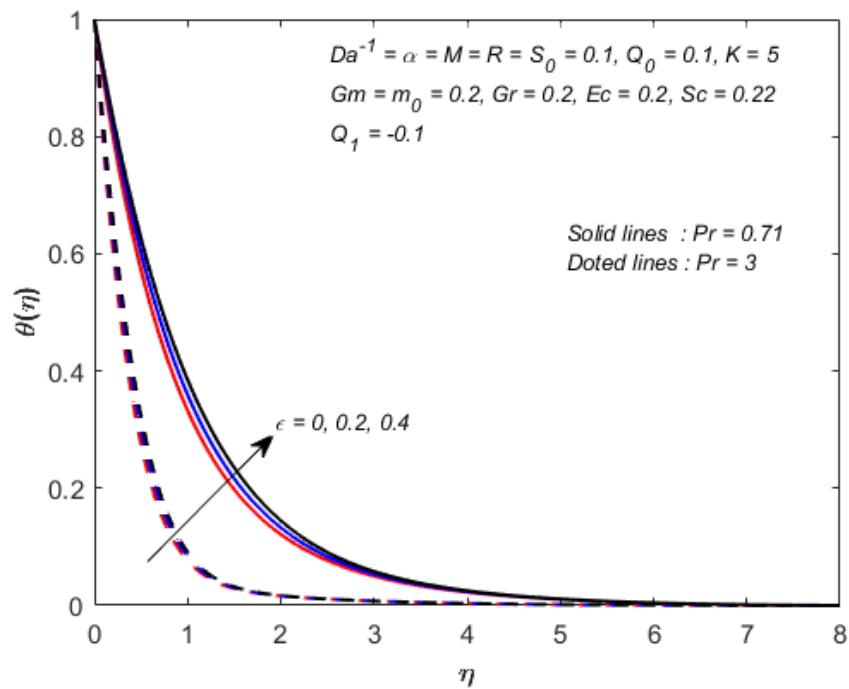


FIGURE 3.10: Impact of ϵ and Pr on temperature $\theta(\eta)$

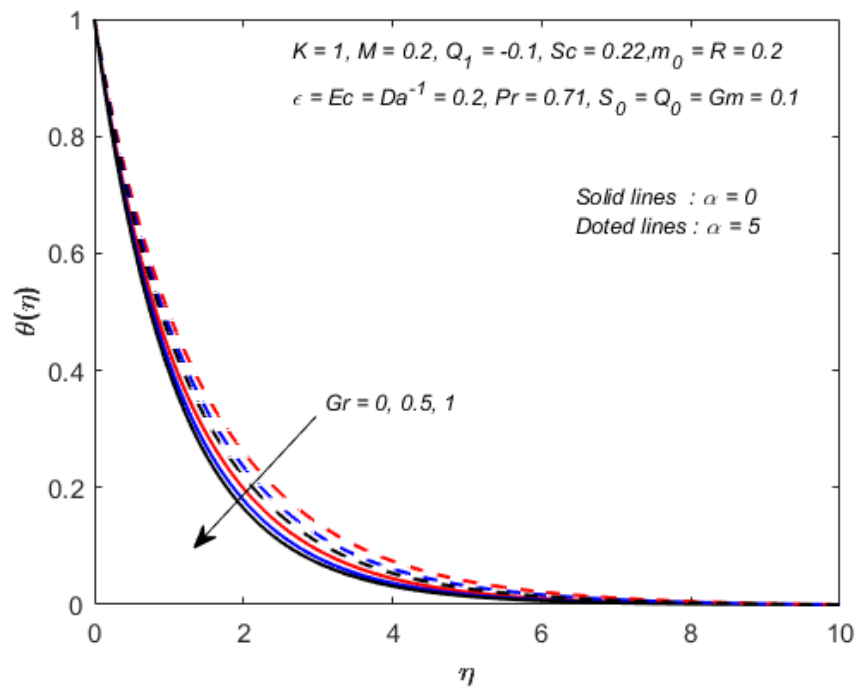


FIGURE 3.11: Impact of Gr and α on temperature $\theta(\eta)$

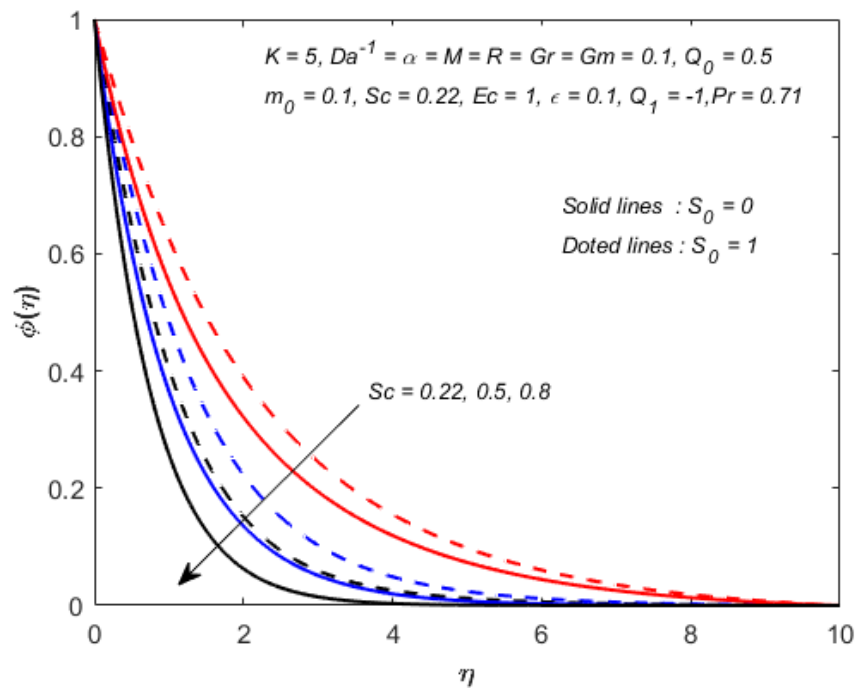
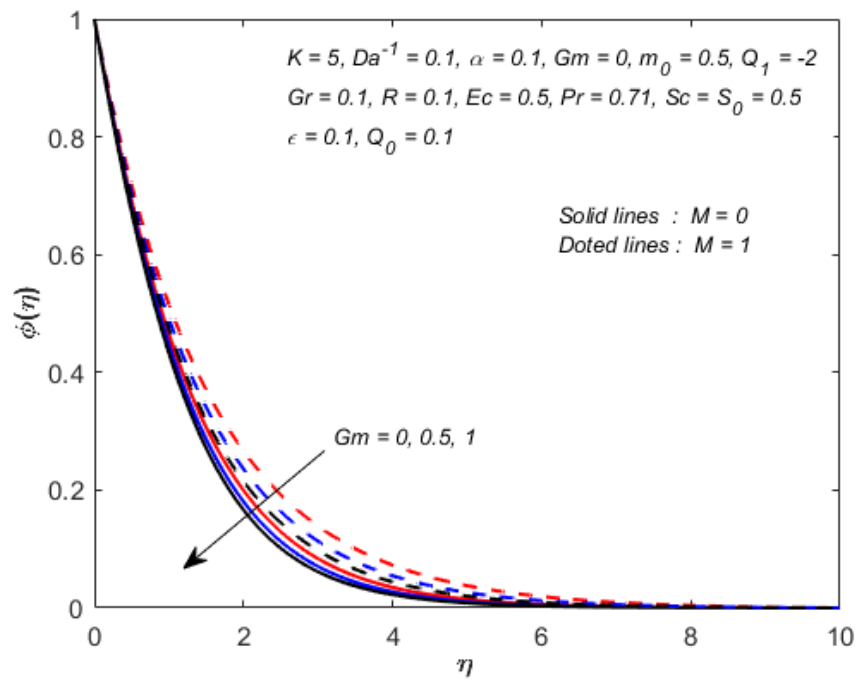


FIGURE 3.12: Impact of Sc and S_0 on the concentration $\phi(\eta)$

FIGURE 3.13: Impact of Gm and M on concentration $\phi(\eta)$

Chapter 4

Non-uniform heat source/sink and activation energy effects on micro polar fluid in the presence of inclined magnetic field and thermal radiation

4.1 Introduction

In the present chapter, some new effects which are not discussed yet in published work of Mabood [38], has been discussed. The effects of inclined magnetic field, Soret and Dufour number and activation energy on the two-dimensional hydro-magnetic mixed convective heat and mass transfer flow of a micropolar fluid over a stretching sheet embedded in a non-Darcian porous medium with thermal radiation have been discussed. The formulated highly non linear equations for the above mentioned flow are converted into first order ODEs. The shooting method is used to solve the BVP by using the computational software MATLAB. A built-in MATLAB function `bvp4c` is accustomed to bolster the numerical results. The

numerical results are computed by choosing different values of the involved physical parameters and compared with the earlier published results. The behaviour of velocity, angular velocity, temperature and concentration, for different physical parameters has been investigated. The graphs and tables which are obtained under this investigation are given and analyzed at the end of this chapter.

4.2 Problem formulation

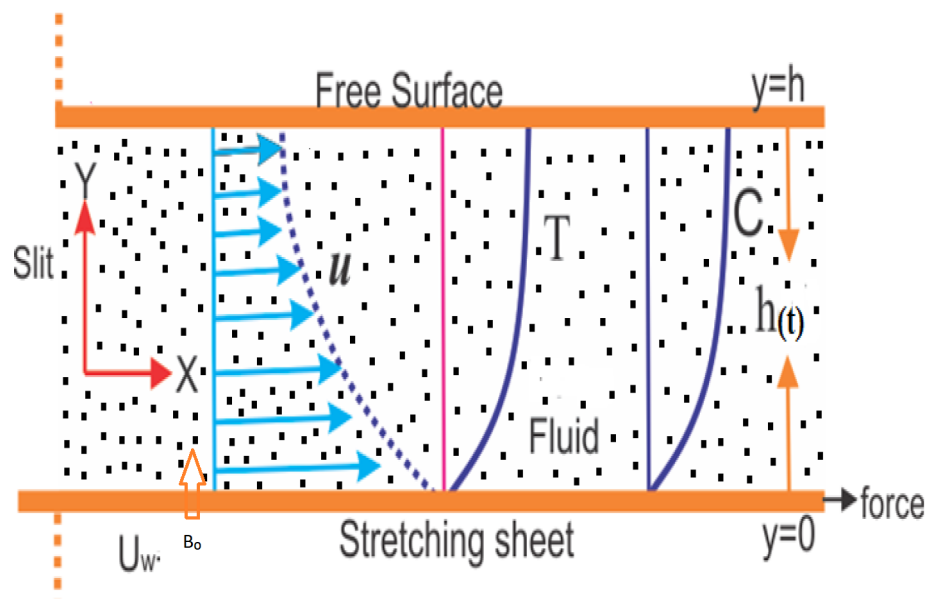


FIGURE 4.1: Geometry for the flow under consideration.

The same flow and conditions which were considered in Chapter 3 are considered here. Extending the idea of Mabood [38], the governing PDEs of the problem stated as ‘MHD convective flow past a stretching sheet in a micropolar fluid with thermal radiation along with activation energy, Dufour effect and inclined magnetic field’ can be written as

$$\frac{\partial u}{\partial x} + \frac{\partial v}{\partial y} = 0, \quad (4.1)$$

$$u \frac{\partial u}{\partial x} + v \frac{\partial u}{\partial y} = \left(\nu + \frac{k_1}{\rho} \right) \frac{\partial^2 u}{\partial y^2} + \frac{k_1}{\rho} \frac{\partial N}{\partial y} - \frac{\nu \varphi}{k} u - \frac{C_b \varphi}{\sqrt{k}} u^2 - \frac{\sigma B_0^2}{\rho} u \sin^2(\beta) + g\beta'(T - T_\infty) + g\beta^*(C - C_\infty). \quad (4.2)$$

$$\rho j \left(u \frac{\partial N}{\partial x} + v \frac{\partial N}{\partial y} \right) = \gamma \frac{\partial^2 N}{\partial y^2} - k_1 \left(2N + \frac{\partial u}{\partial y} \right), \quad (4.3)$$

$$u \frac{\partial T}{\partial x} + v \frac{\partial T}{\partial y} = \frac{1}{\rho C_p} \frac{\partial}{\partial y} \left(K \frac{\partial T}{\partial y} \right) - \frac{1}{\rho C_p} \frac{\partial q_r}{\partial y} + \frac{\sigma B_0^2}{\rho C_p} u^2 \sin^2(\beta) + \frac{q'''}{\rho C_p} + \frac{\mu}{\rho C_p} \left(\frac{\partial u}{\partial y} \right)^2 \quad (4.4)$$

$$+ \frac{D_m k_T}{C_s C_p} \frac{\partial^2 C}{\partial y^2},$$

$$u \frac{\partial C}{\partial x} + v \frac{\partial C}{\partial y} = D_m \frac{\partial^2 C}{\partial y^2} + \frac{D_m k_T}{T_m} \frac{\partial^2 T}{\partial y^2} - k_r^2 (C - C_\infty) \left(\frac{T}{T_\infty} \right)^n e^{-\frac{E_a}{kT}}. \quad (4.5)$$

The term $k_r^2 (C - C_\infty) \left(\frac{T}{T_\infty} \right)^n e^{-\frac{E_a}{kT}}$ represents the Arrhenius equation, where k_r is reaction rate, E_a the activation energy, k is Boltzmann constant and n is the fitted rate constant. β is the inclination angle of magnetic field. The corresponding BCs for the proposed model are

$$\left. \begin{aligned} u = u_w = bx, \quad v = 0, \quad N = -m \frac{\partial u}{\partial y}, \quad T = T_w = T + A_0 \left(\frac{x}{l} \right)^2, \\ C = C_w = C + A_1 \left(\frac{x}{l} \right)^2 \quad \text{at } y = 0, \\ u \rightarrow 0, \quad N \rightarrow 0, \quad T \rightarrow T_\infty, \quad C \rightarrow C_\infty \quad \text{as } y \rightarrow \infty. \end{aligned} \right\} \quad (4.6)$$

where x and y are coordinate axis along the continuous surface in the direction same as direction of motion and normal to it, respectively. The components of velocity along x - and y -axis are respectively u and v .

4.3 Dimensionless form of the model

To solve the above system of PDEs numerically, we first convert it into the non-dimensionalized form. For this we use the following dimensionless variables:

$$\left. \begin{aligned} \eta &= \sqrt{\frac{b}{\nu}}y, \quad N = bx\sqrt{\frac{b}{\nu}}g(\eta), \quad u = bx f'(\eta), \quad v = \sqrt{b\nu}f(\eta), \quad \theta(\eta) = \frac{T - T_\infty}{T_w - T_\infty}, \\ \phi(\eta) &= \frac{C - C_\infty}{C_w - C_\infty}, \\ T - T_\infty &= A_0 \left(\frac{x}{l}\right)^2 \theta(\eta), \quad T_w - T_\infty = A_0 \left(\frac{x}{l}\right)^2, \quad C - C_\infty = A_1 \left(\frac{x}{l}\right)^2 \phi(\eta), \\ C_w - C_\infty &= A_1 \left(\frac{x}{l}\right)^2. \end{aligned} \right\} \quad (4.7)$$

where f and g are the stream and microrotation functions respectively and both are dimensionless, η is the similarity variable, l is the characteristic length. The above, equation (4.1) is satisfied identically. Remaining governing Eqs are transformed into the following form:

$$(1 + K)f''' + ff'' - (f')^2 - Da^{-1}f' - \alpha(f')^2 + kg' - Mf' \sin^2(\beta) + Gr\theta + Gm\phi = 0, \quad (4.8)$$

$$\left(1 + \frac{K}{2}\right)g'' - K(2g + f'') - f'g + fg' = 0, \quad (4.9)$$

$$(1 + R + \epsilon\theta)\theta'' + Pr(f\theta' - 2f'\theta) + \epsilon(\theta')^2 + PrMEc(f')^2 \sin^2(\beta) + PrEc(f'')^2 \quad (4.10)$$

$$\begin{aligned} &+ (1 + \epsilon\theta)(Q_0f' + Q_1\theta) \\ &+ Pr D_f \phi'' = 0, \end{aligned} \quad (4.11)$$

$$\phi'' + Sc(\phi'f - 2\phi f') + ScS_0\theta'' - Sc\sigma(1 + \delta\theta)^n e^{\frac{-E}{1+\delta\theta}}. \quad (4.12)$$

The BCs, now, become:

$$f(\eta) = 0, \quad f'(\eta) = 1, \quad g(\eta) = -m_0 f''(\eta), \quad \theta(\eta) = 1, \quad \phi(\eta) = 1 \quad \text{at } \eta = 0, \quad (4.13)$$

$$f'(\eta) \rightarrow 0, \quad g(\eta) \rightarrow 0, \quad \theta(\eta) \rightarrow 0, \quad \phi(\eta) \rightarrow 0, \quad \text{as } \eta \rightarrow \infty. \quad (4.14)$$

The dimensionless parameters are defined as

$$\left. \begin{aligned} Da^{-1} &= \frac{\phi\nu}{kb}, \quad M = \frac{\sigma}{\rho b} B_0^2, \quad Gr = \frac{g\beta'(T - T_\infty)}{b^2 l}, \quad G_m = \frac{g\beta^*(C - C_\infty)}{b^2 l}, \quad K = \frac{k_1}{\mu}, \\ E_c &= \frac{b^2 l}{A_0 C_p}, \quad R = \frac{16T_\infty^3 \sigma^*}{3k^* k_\infty}, \quad Sc = \frac{\nu}{D_m}, \quad S_0 = \frac{k_T (T_w - T_\infty)}{T_m (C_w - C_\infty)}, \quad Pr = \frac{\mu C_p}{K_\infty}. \end{aligned} \right\} \quad (4.15)$$

The skin-friction coefficient C_f , Nusselt number Nu_x and Sherwood number Sh_x are defined as

$$C_f = \frac{\tau_w}{\rho u_w^2}, \quad Nu_x = \frac{xq_w}{k(T_w - T_\infty)}, \quad Sh_x = \frac{xm_w}{D_m(C_w - C_\infty)}. \quad (4.16)$$

Here, the heat flux q_w , the skin-friction on flat plate τ_w , and the mass transfer rate m_w are given by

$$\tau_w = \left(|\mu + k_1| \frac{\partial u}{\partial y} \right)_{y=0}, \quad q_w = -K \left(\frac{\partial T}{\partial y} \right)_{y=0}, \quad m_w = -D_m \left(\frac{\partial C}{\partial y} \right)_{y=0}. \quad (4.17)$$

By using the above equations, we have

$$C_f Re_x^{1/2} = (1 + K)f'(0), \quad Nu_x = -\sqrt{Re_x}\theta(0), \quad Sh_x = -\sqrt{Re_x}\phi(0). \quad (4.18)$$

Here, $Re_x = \frac{u_w x}{\nu}$ is the local Reynolds number.

4.4 Numerical Treatment

This section is focused on the implementation of the shooting method to solve the transformed ODEs (4.8)-(4.11) subject to the boundary conditions (4.12)-(4.13). For this purpose, we first convert the system of ODEs into first order ODEs, by using the following notations by using the following notations

$$f = y_1, \quad f' = y_2, \quad f'' = y_3, \quad g = y_4, \quad g' = y_5, \quad \theta = y_6, \quad \theta' = y_7, \quad \phi = y_8, \quad \phi' = y_9. \quad (4.19)$$

The resulting system of first order ODEs is:

$$\begin{aligned}
y_1' &= y_2, \\
y_2' &= y_3, \\
y_3' &= \left(\frac{1}{1+K} \right) (-y_1 y_3 + y_2^2 + Da^{-1} y_2 + \alpha y_2^2 - k y_5 + M y_2 - Gr y_6 - G m y_8), \\
y_4' &= y_5, \\
y_5' &= \frac{2}{2+K} (K(2y_4 + y_3) + y_2 y_4 - y_1 y_5), \\
y_6' &= y_7, \\
y_7' &= \frac{1}{(1+R+\epsilon y_6)} (-Pr(y_1 y_7 - 2y_2 y_6) - \epsilon y_7^2 - PrMEcy_2^2 - PrEcy_3^2 - \\
&(1+\epsilon y_6)(Q_0 y_2 + Q_1 y_6) \\
&- PrD_f y_9'), \\
y_8' &= y_9, \\
y_9' &= -Sc(y_9 y_1 - 2y_8 y_2 + S_0 y_7') + Sc\sigma(1+\delta y_6)^n e^{\frac{-E}{1+\delta y_6}}.
\end{aligned}$$

The resulting form of the boundary conditions is

$$\begin{aligned}
y_1(0) &= 0, \quad y_2(0) = 1, \quad y_4(0) = -m_0 y_3(0), \quad y_6(0) = 1, \quad y_8(0) = 1, \\
y_2 &\rightarrow 0, \quad y_4 \rightarrow 0, \quad y_6 \rightarrow 0, \quad y_8 \rightarrow 0 \quad \text{as } \eta \rightarrow \infty.
\end{aligned}$$

To solve these equations numerically, the unbounded domain $[0, \infty)$ is replaced by an appropriate domain $[0, \eta_{max}]$. To solve the above ODEs by the shooting method, the initial values of $y_3(0)$, $y_5(0)$, $y_7(0)$, $y_9(0)$ are chosen arbitrarily. During the execution of iterations these initial guesses will be updated by the Newton's method and the process will be continued until the following criteria is met

$$\max\{|y_2(\eta_{max}) - 0|, |y_4(\eta_{max}) - 0|, |y_6(\eta_{max}) - 0|, |y_8(\eta_{max}) - 0|\} < (10)^{-5}$$

4.5 Results and discussion

For the validity of our MATLAB code, the skin friction factor and the local Nusselt number have been compared with those already published in literature as shown in Tables 4.1 and 4.2.

TABLE 4.1: Impact of different values of K on $C_f Re_x^{1/2}$ keeping all other parameters zero

K	[46]	[38]	Current Results
0	-1.000000	-1.000008	-1.0000083
1	-1.367872	-1.367996	-1.3679962
2	-1.621225	-1.621575	-1.6215750
3	-	-1.827382	-1.8273821
4	-2.004133	-2.005420	-2.0054202
5	-	-2.164823	-2.1648229

TABLE 4.2: Impact of different values of Pr on $C_f Re_x^{1/2}$ keeping all other parameters zero

Pr	[47]	[48]	[19]	[23]	[38]	Current Results
1	1.3333	1.33334	1.3333	1.333333	1.33333334	1.33333334
3	2.5097	2.50997	2.5097	2.509725	2.50972157	2.50972157
10	4.7969	4.79686	4.7969	4.796873	4.79687059	4.79687058

From tables it can be seen that the results achieved by the present code are found convincingly very closed to the published results.

Fig. 4.2 represents the velocity profile for different values of K and M while all other parameters are kept constant. We can see from this figure that as the value of M is ascalated the velocity profile declined and a reverse scenario is observed in the case of material parameter K . The velocity is decreased by increasing the values of M because of an opposite force named as the Lorentz force, which

has the tendency to reduce the velocity. Figure 4.3 divulges the velocity profile for changing values of Da^{-1} and m_0 while all other parameters are kept constant. Figure shows that the velocity profile gets sharper for increasing value of Da^{-1} and m_0 . In Figure, 4.4 it can be seen that as we increase the values of K and M , the angular velocity increases while all other parameters have the fixed values. Figure 4.5 divulges that as we increase the values of Da^{-1} and m_0 , the angular velocity increases near the wall while all other parameters have fixed values. Figure 4.6 delineates the effect of Q_0 and R on the dimensionless temperature profile $\theta(\eta)$. It is found that with the increasing values of Q_0 and R , the thermal boundary layer thickness increases. An increment in Q_0 allows the flow to become more energetic, this increment in energy increases the overall temperature of the fluid. Figure 4.7 depicts the behaviour of the dimensionless temperature $\theta(\eta)$ which escalates with escalation of M and declines with the declination of Q_1 . As we increase M , the opposite Lorentz force comes into act which offers resistance to the flow and thus the thermal boundary layer thickness is increased. Figure 4.8 depicts the behaviour of the dimensionless temperature $\theta(\eta)$ which is observed to increase with an augmentation in the Ec and decrease for increasing values of K . The physical reason behind it is that an increment in the dissipation enhances the thermal conductivity of the fluid which causes an enhancement in the thermal boundary layer. It is clear from Figure 4.9 that if we increase the inverse Darcy number and constant number m_0 the value of $\theta(\eta)$ increases. In Figure 4.10 it has been illustrated that the temperature profile increases as the physical parameter ϵ increases and decreases with an increment in Pr . This is because when we increase the Prandtl number Pr , heat diffuses casually away from the sheet, as a result the temperature and the thermal boundary layer thickness reduce. Figure 4.11 demonstrates the influence of Grashof number Gr and local inertia-coefficient α on temperature profile. Here $\theta(\eta)$ is direct in proportion with α and inverse in proportion with Gr . Figure 4.12 is the illustration of dimensionless concentration with varying values of S_0 and Sc . We can see that $\phi(\eta)$ escalate as S_0 escalate and decline as Sc escalate. Physically Sc is the ratio of momentum to mass diffusivities, so for larger Sc mass diffusivity reduces which causes decadence in

ϕ . Figure 4.13 is the illustration of dimensionless concentration with varying values of Gm and M . We can see that $\phi(\eta)$ escalate as M escalate and decline as Gm escalate. Figure 4.14 portray the effect of σ and K on $\theta\eta$. From figure we can see that the rising value of σ leads to the reduction in $\theta\eta$ with the steep gradient near the wall. Also $\theta\eta$ declines as K escalate. Figure 4.15 showing the concentration profile for δ and M . Declination of concentration has been observed for the escalation of δ and the same behaviour is observed for M . This is because when temperature increases the volume of the fluid increases thus concentration terms decrease. In Figure 4.16, declination of concentration is observed for the escalation of n and a reverse scenario is observed in the case of material parameter K . In flow under consideration the rate law is first order therefore we analyse the behaviour for values less than (1) and concentration is inversely proportional to fitted rate constant. Figure 4.17 presents the change of $\theta(\eta)$ for Df and M . Clearly increasing values of M corresponds to the increasing values of $\theta(\eta)$. Figure also shows that escalation of Df escalates $\theta(\eta)$. Higher concentration gradient is observed on increasing Df . This is because the Dufour effect is pointed about the point of energy flux generation by composition gradient. The influence of magnetic field at different orientations has been displayed in figs. 4.18, 4.19, 4.20. From figures it is pretty clear that as we increase the inclination angle fluid flow falls down. This behaviour is observed due to the reason that usually when magnetic field is applied it offers maximum resistance as compared to applying it at certain angle. Hence in the presence of differently oriented magnetic field the velocity decreases but temperature and concentration increases. On the other hand as K and n are escalated the temperature and concentration declined respectively, While velocity increases on increasing values of K .

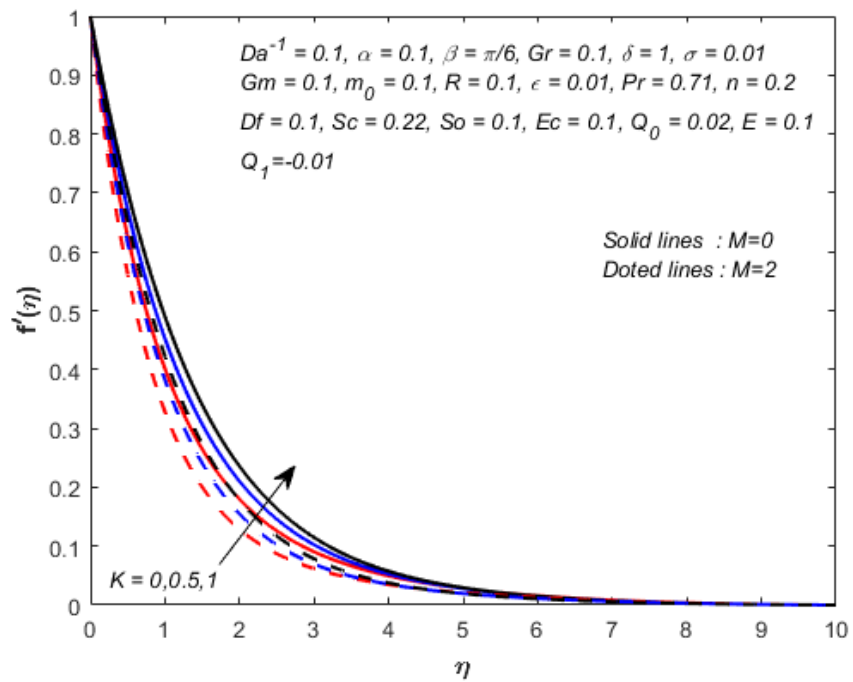


FIGURE 4.2: Impact of K and M on velocity $f'(\eta)$

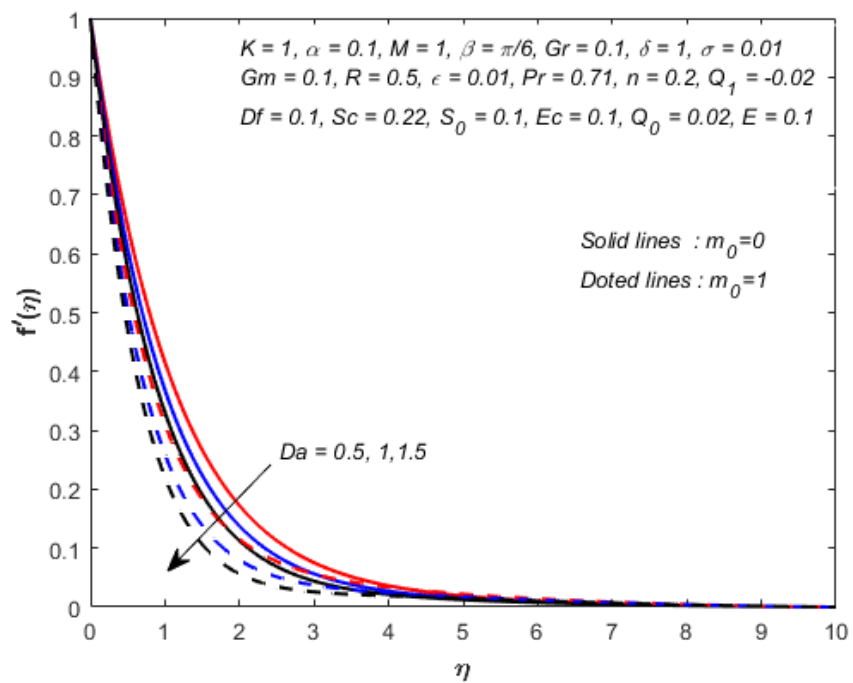


FIGURE 4.3: Impact of Da^{-1} and m_0 on the velocity $f'(\eta)$

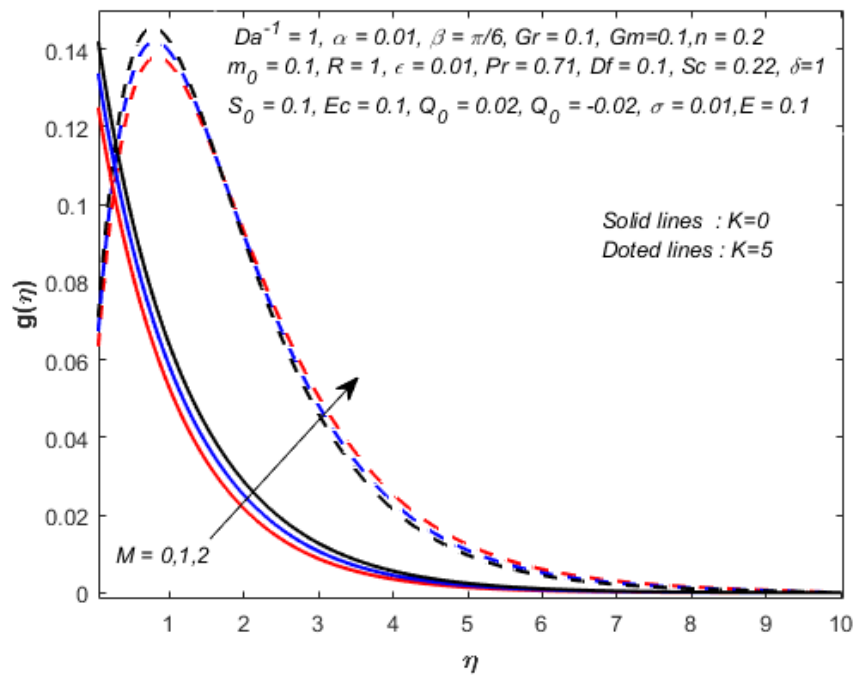


FIGURE 4.4: Impact of M and K on angular velocity $g(\eta)$

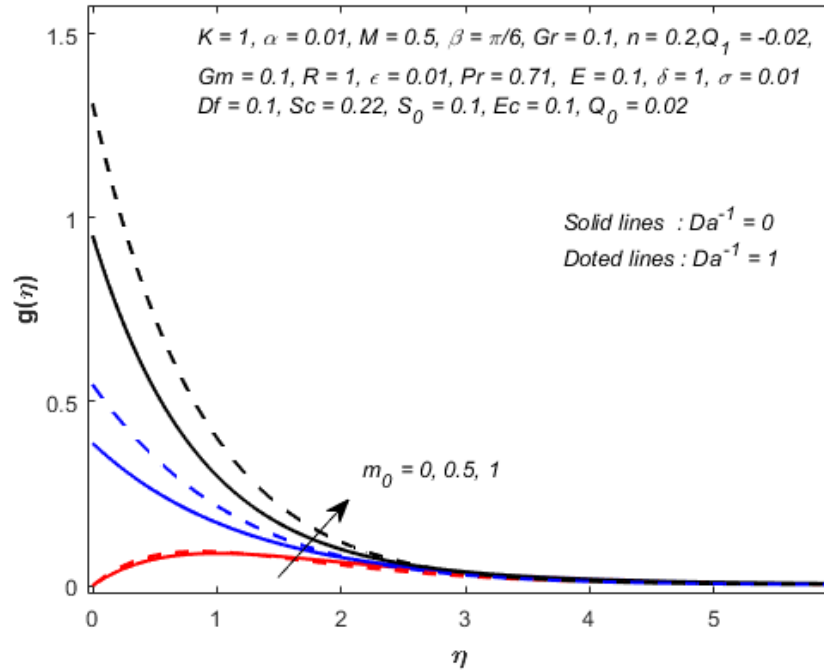
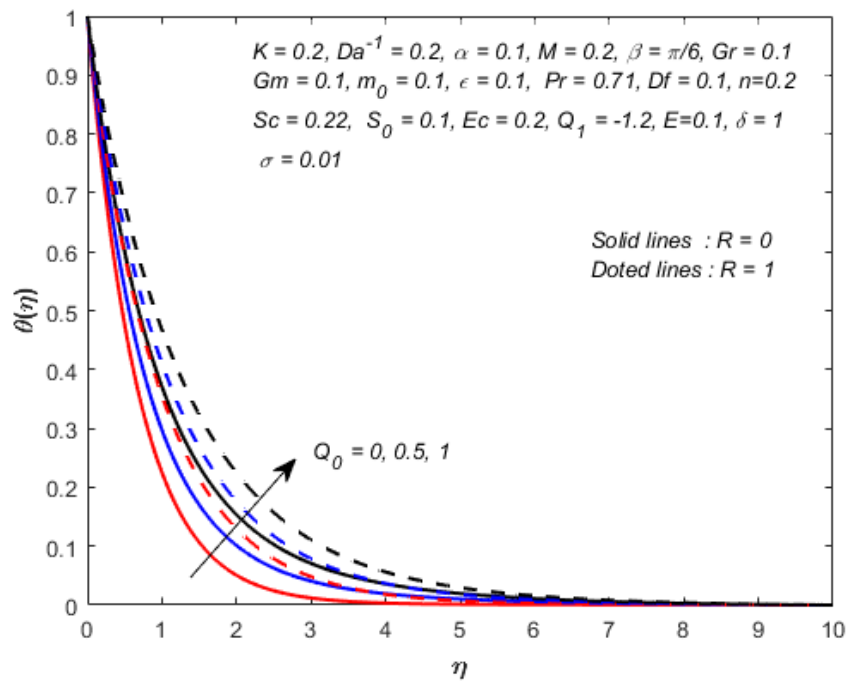
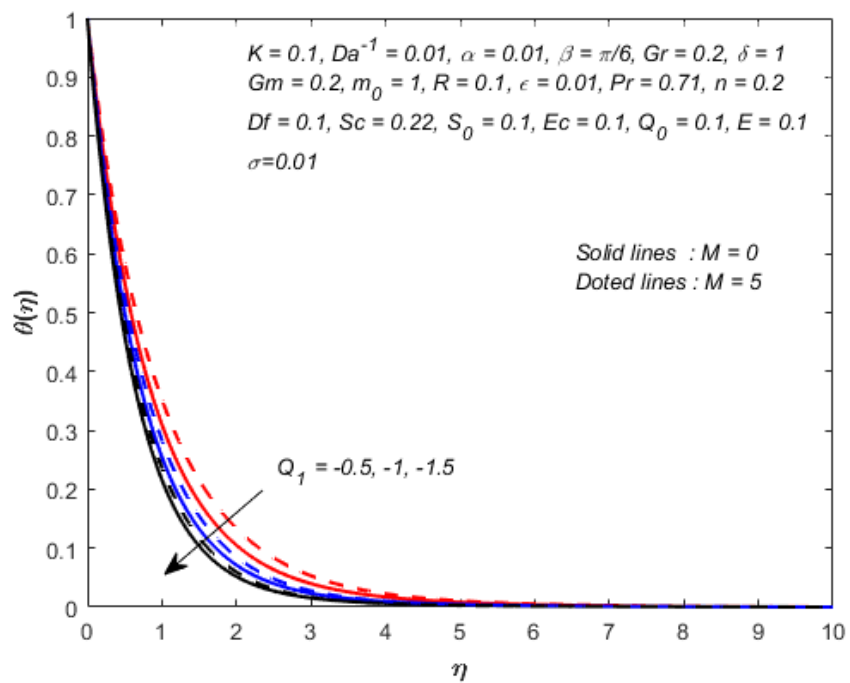
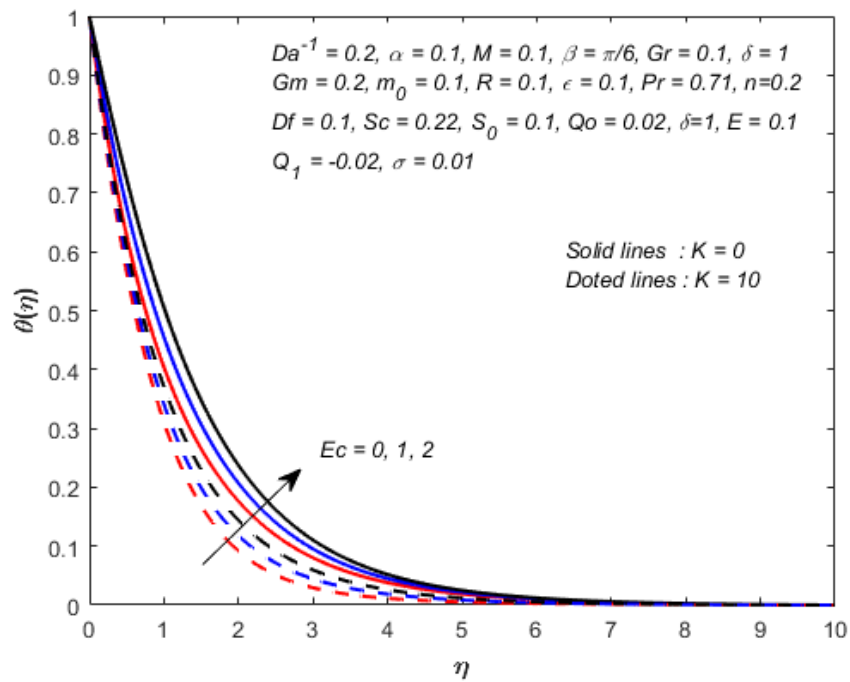
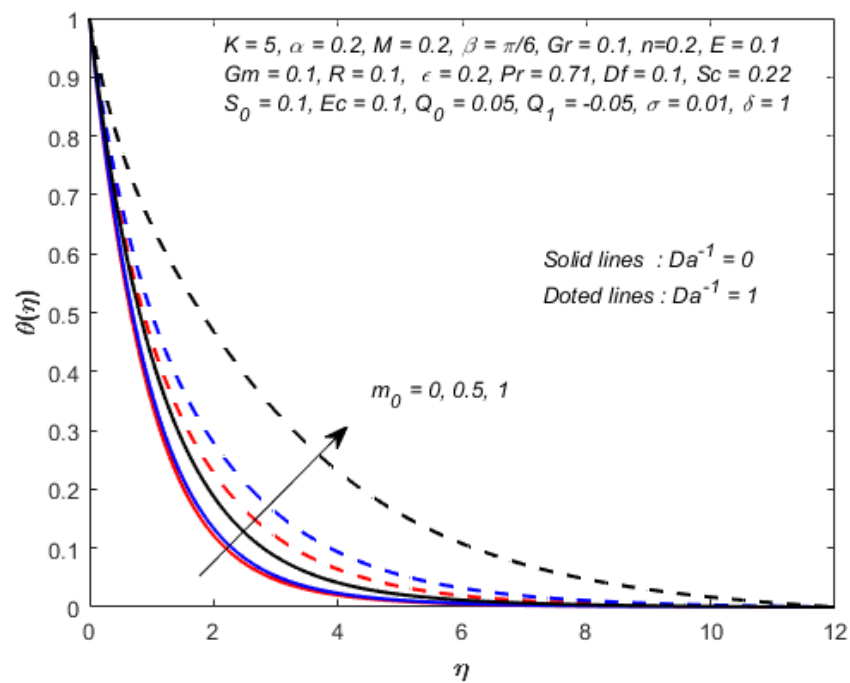


FIGURE 4.5: Impact of m_0 and Da^{-1} on angular velocity $g(\eta)$

FIGURE 4.6: Impact of R and Q_0 on temperature $\theta(\eta)$ FIGURE 4.7: Impact of Q_1 and M on temperature $\theta(\eta)$

FIGURE 4.8: Impact of Ec and K on temperature $\theta(\eta)$ FIGURE 4.9: Impact of m_0 and Da^{-1} on temperature $\theta(\eta)$

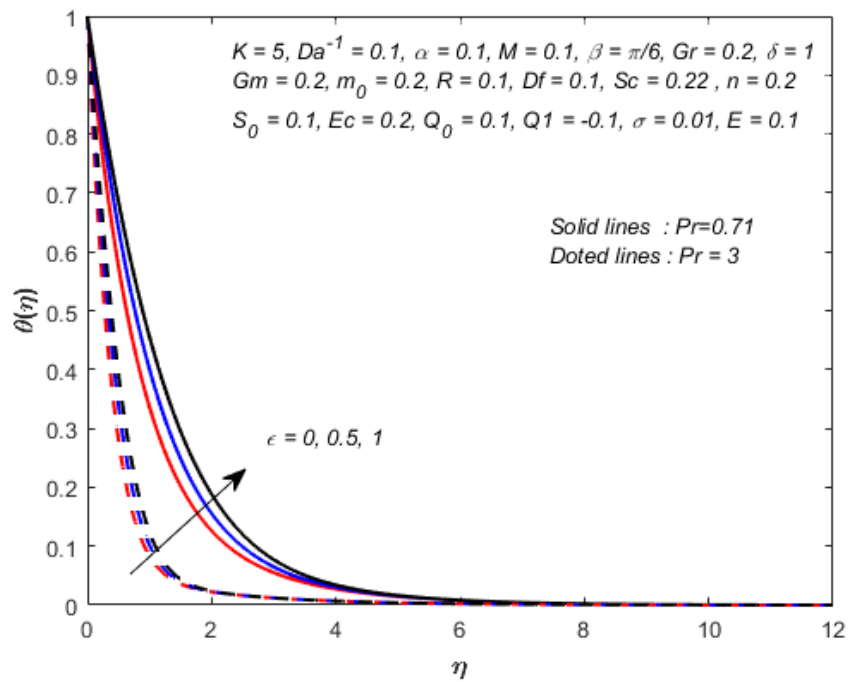


FIGURE 4.10: Impact of ϵ and Pr on temperature $\theta(\eta)$

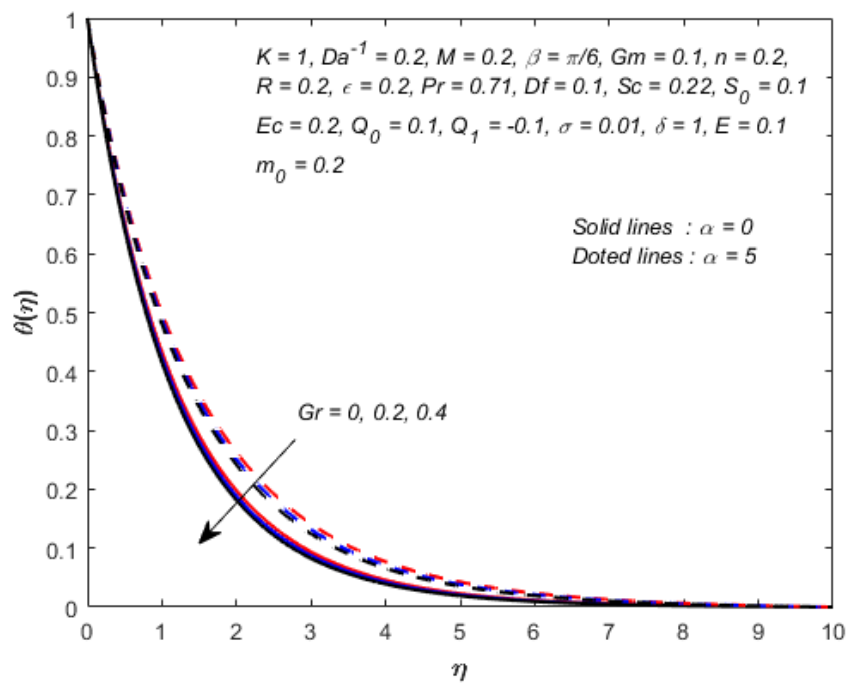


FIGURE 4.11: Impact of Gr and α on temperature $\theta(\eta)$

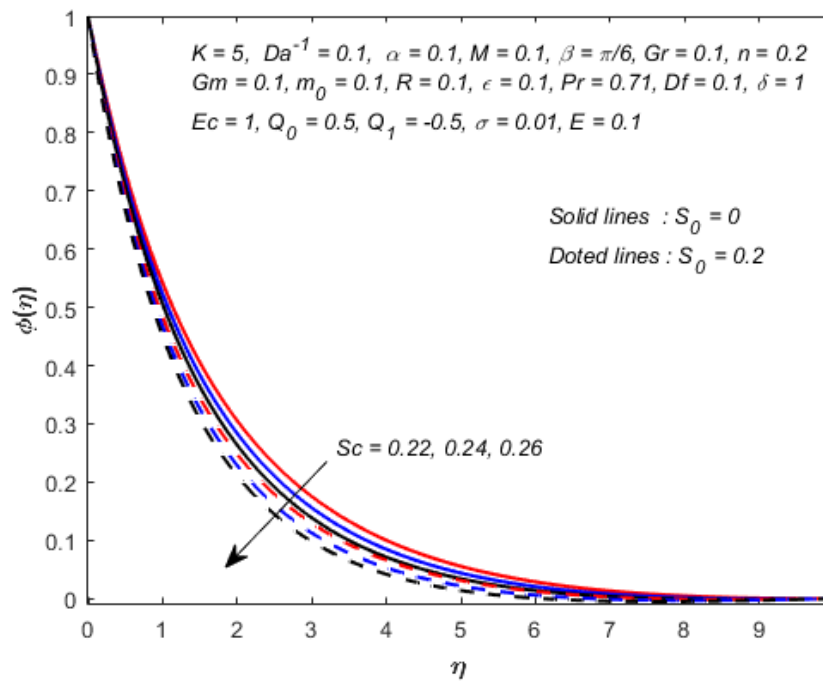


FIGURE 4.12: Impact of Sc and S_0 on the concentration $\phi(\eta)$

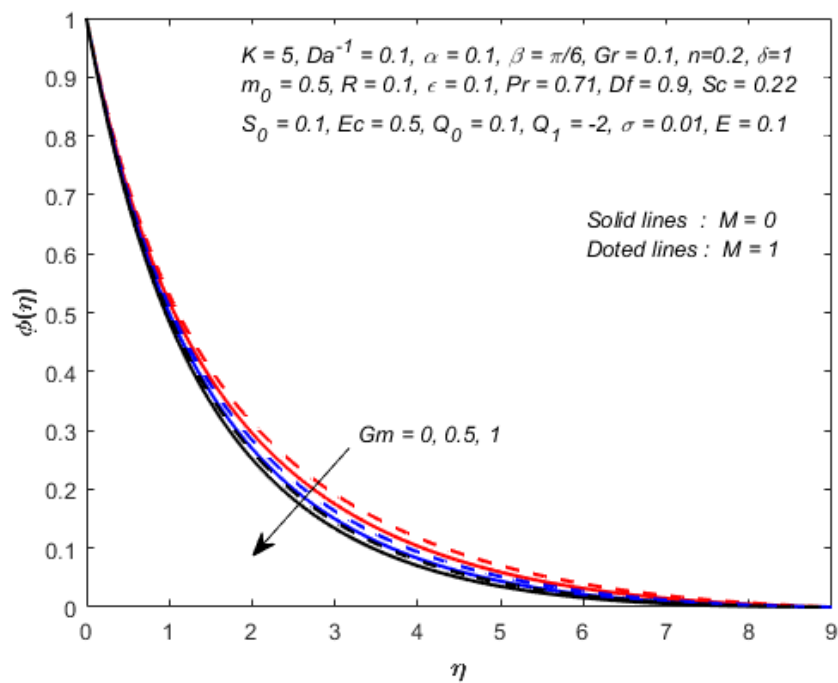
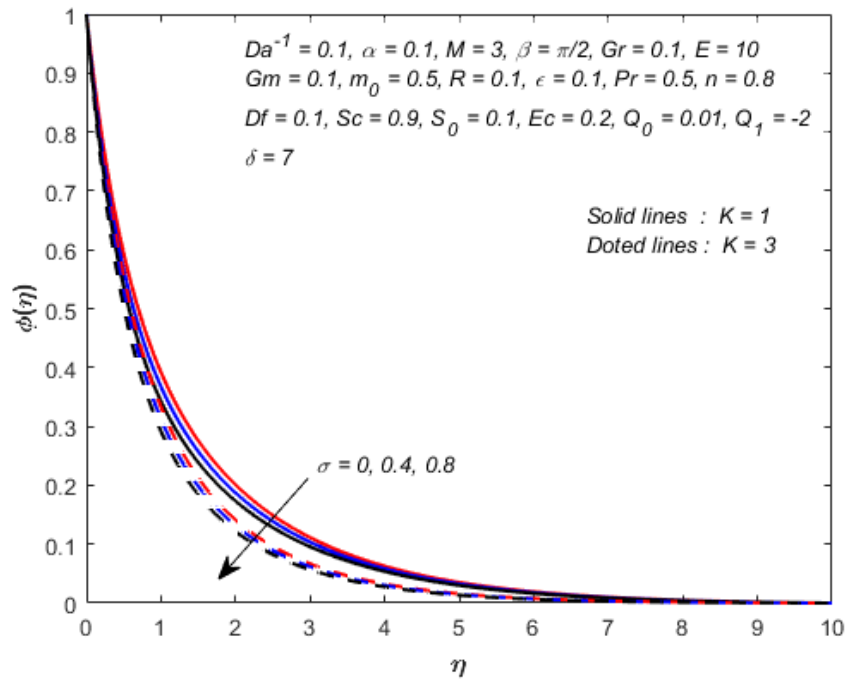
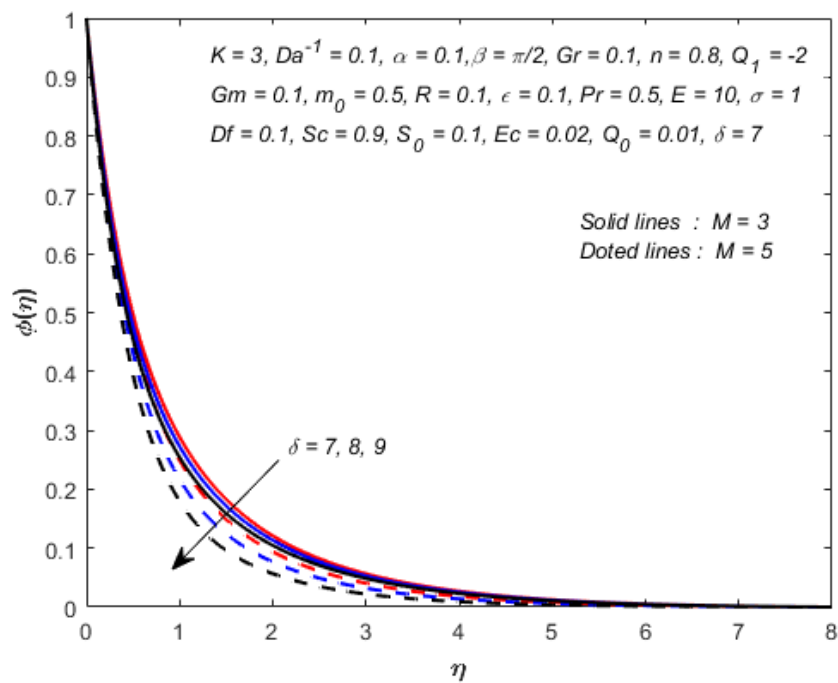


FIGURE 4.13: Impact of Gm and M on concentration $\phi(\eta)$

FIGURE 4.14: Impact of σ and K on concentration $\phi(\eta)$ FIGURE 4.15: Impact of δ and M on concentration $\phi(\eta)$

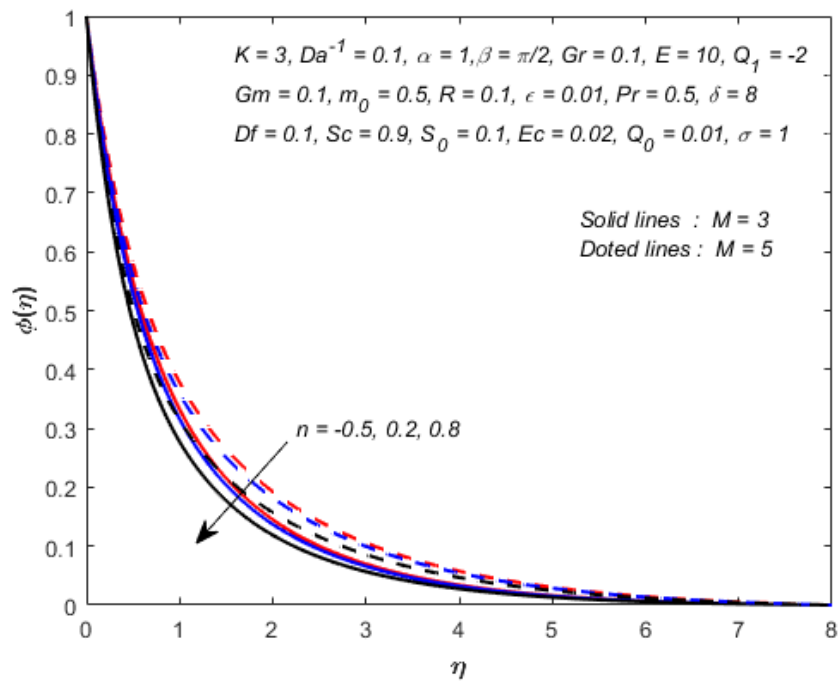


FIGURE 4.16: Impact of n and M on concentration $\phi(\eta)$

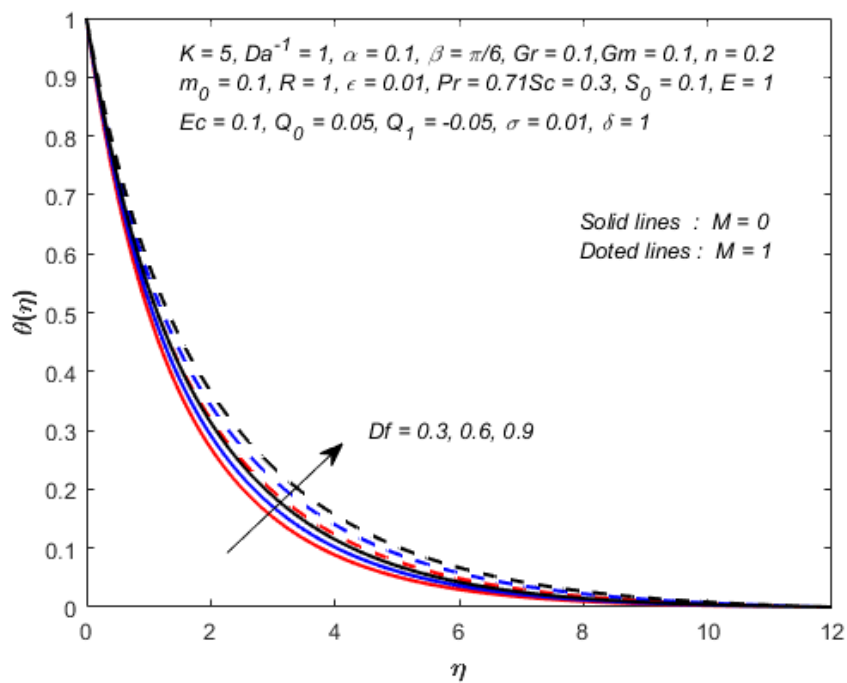


FIGURE 4.17: Impact of Df and M on concentration $\phi(\eta)$

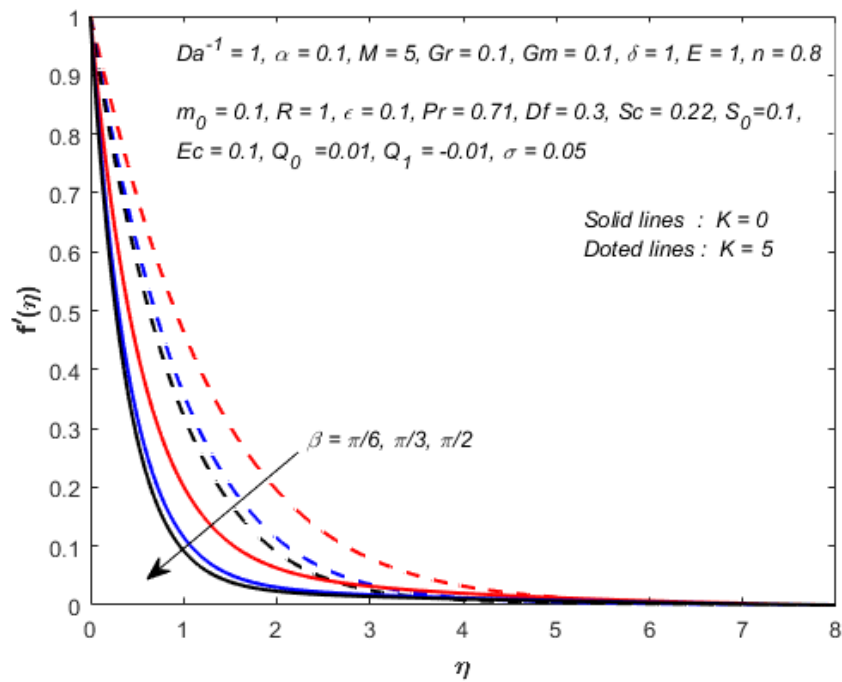


FIGURE 4.18: Impact of β and K on velocity $f'(\eta)$

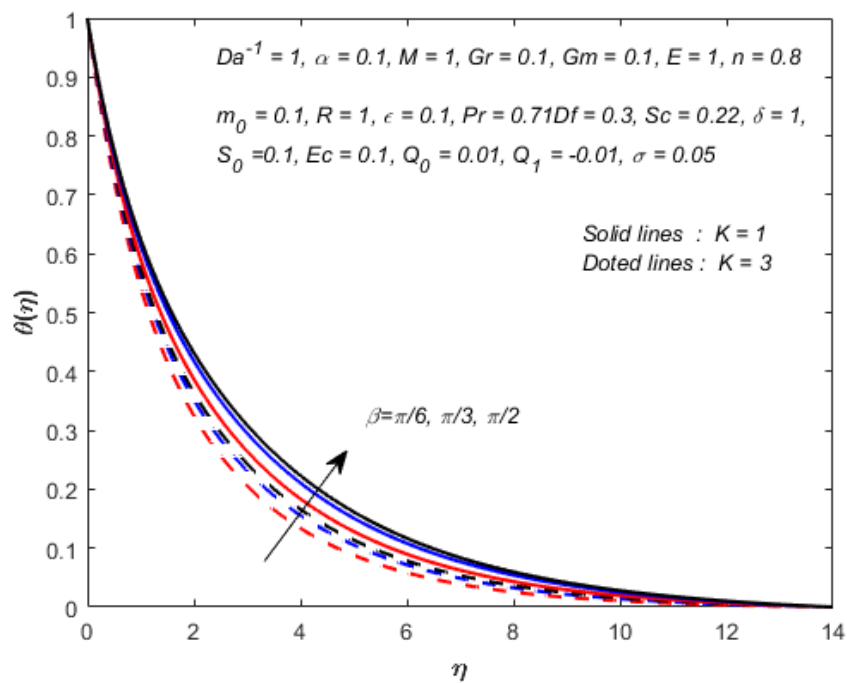
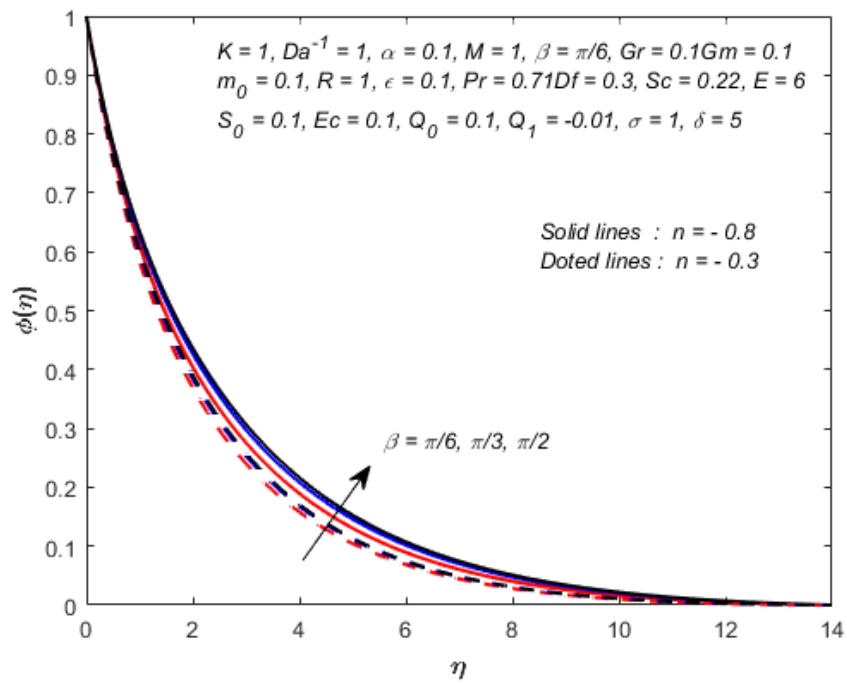


FIGURE 4.19: Impact of β and K on temperature $\theta(\eta)$

FIGURE 4.20: Impact of β and n on concentration $\phi(\eta)$

Chapter 5

Conclusion

Our thesis presents the non-uniform heat source/sink and activation energy effects on micropolar fluid in the presence of inclined magnetic field and thermal radiation. An MHD flow over a stretching sheet is discussed alongwith the Dufour number and the Soret number effects. The shooting method is used to solve the BVP by using the computational software MATLAB. A built-in MATLAB function `bvp4c` is accustomed to bolster the numerical results. The behaviour of velocity, temperature, concentration and angular velocity for different physical parameters have been investigated. The results are also elaborated in graphical and tabular form. Following conclusions have been drawn from the numerical results.

- The concentration profile declines by the escalation of the fitted rate constant n , the chemical reaction rate σ and the temperature difference parameter δ .
- In the presence of differently oriented magnetic field the velocity decreases but the temperature and the concentration increase.
- A higher concentration is observed on increasing the Dufour number. Also escalation of Df escalates the temperature profile.
- The angular velocity escalates with the escalation in m_0 , the material parameter K , the inverse Darcy number Da^{-1} and the magnetic field parameter M .

- The rate of mass transfer escalates with Soret number and declines with the escalation of Schmidt number.
- The velocity and the concentration escalate by the escalation in the modified Grashof number Gm and the thermal Grashof number Gr and a reverse scenario is observed in the temperature field.

Bibliography

- [1] M. M. Bhatti and M. M. Rashidi, “Study of heat and mass transfer with joule heating on magnetohydrodynamic(mhd) peristaltic blood flow under the influence of hall effect,” *Propulsion and Power Research*, 2016.
- [2] S. P. A. Devi and B. Ganga, “Effects of viscous and joules dissipation on mhd flow, heat and mass transfer past a stretching porous surface embedded in a porous medium,” *Nonlinear Analysis: Modelling and Control*, vol. 14, no. 3, pp. 303–314, 2009.
- [3] C. S. K. Raju, N. Sandeep, V. Sugunamma, J. Jayachandra Babu, and J. V. Ramana Reddy, “Heat and mass transfer in magnetohydrodynamic casson fluid over an exponentially permeable stretching surface,” *Engineering Science and Technology, an International Journal*, vol. 19, pp. 45–52, 2016.
- [4] T. Ariman, M. A. Turk, and N. D. Sylvester, “Microcontinuum fluid mechanics areview,” *International Journal of Engineering Science*, vol. 11, no. 8, pp. 905–930, 1973.
- [5] T. Ariman, N. D. Sylvester, and M. A. Turk, “Application of microcontinuum fluid mechanics,” *International Journal of Engineering Science*, vol. 12, no. 4, pp. 273–293, 1974.
- [6] G. Lukaszewicz, “Micropolar fluids: Theory and application,,” *Book*, 1999.
- [7] A. C. Eringen, “Theory of micropolar fluids,” *Journal of Mathematics and Mechanics*, vol. 16, no. 1, pp. 1–18, 1966.

-
- [8] A. C. Eringen., “Theory of micropolar fluids,” *Journal of Mathematical Analysis and Applications*, vol. 38, no. 2, pp. 480–496, 1972.
- [9] A. Eringen, “Microcontinuum field theories, ii: Fluent media,” *Book*, 2001.
- [10] M. A. Mansour, M. A. El-Hakiem, and S. M. El Kabeir, “Heat and mass transfer in magnetohydrodynamic flow of micropolar fluid on a circular cylinder with uniform heat and mass flux,” *Journal of Magnetism and Magnetic Materials*, vol. 220, pp. 259–270, 2000.
- [11] M. A. El-Hakiem, “Viscous dissipation effects on mhd free convection flow over a nonisothermal surface in a micro polar fluid,” *International Communications in Heat and Mass Transfer*, vol. 27, pp. 581–590, 2000.
- [12] M. M. El-Hakiem, A. A. Mohammadein, and S. M. M. El-Kabeir, “Joule heating effects on magneto hydrodynamic free convection flow of a micro polar fluid,” *International Communications in Heat and Mass Transfer*, vol. 26, pp. 219–227, 1999.
- [13] M. F. El-Amin, “Magnetohydrodynamic free convection and mass transfer flow in micropolar fluid with constant suction,” *Journal of Magnetism and Magnetic Materials*, vol. 234, pp. 567–574, 2011.
- [14] G. Deepa and G. Murali, “Effects of viscous dissipation on unsteady mhd free convective flow with thermophoresis past a radiate inclined permeable plate,” *Iranian Journal of Science and Technology.*, vol. 38, pp. 379–388, 2014.
- [15] E. M. Abo-eldohad and A. F. Ghonaim, “Radiation effect on heat transfer of a micropolar fluid through a porous medium,” *Applied Mathematics and Computation*, vol. 169, pp. 500–516., 2005.
- [16] M. M. Rahman and T. Sultana, “Radiative heat transfer flow of micropolar fluid with variable heat flux in a porous medium.” *Nonlinear Analysis: Modelling and Control*, vol. 13, no. 1, pp. 71–87, 2008.

-
- [17] M. A. A. Mahmoud, “Thermal radiation effects on mhd flow of a micropolar fluid over a stretching surface with variable thermal conductivity,” *Physics A.*, vol. 375, pp. 401–410, 2007.
- [18] A. J. Chamkha, R. A. Mohamed, and S. E. Ahmed, “Unsteady mhd natural convection from a heated vertical porous plate in a micropolar fluid with joule heating, chemical reaction and radiation effects,,” *Meccanica.*, vol. 46, pp. 399–411, 2011.
- [19] A. Ishak, “Thermal boundary layer flow over a stretching sheet in a micropolar fluid with radiation effect,” *Meccanica.*, vol. 45, pp. 367–373, 2010.
- [20] F. S. Ibrahim, A. M. Elaiw, and A. A. Bakr, “Influence of viscous dissipation and radiation on unsteady mhd mixed convection flow of micropolar fluids,” *Applied Mathematics and Information Sciences.*, vol. 2, pp. 143–162, 2008.
- [21] M. M. Rashidi, S. A. Mohimani pour, and S. Abbasbandy, “Analytic approximate solutions for heat transfer of a micropolar fluid through a porous medium with radiation,” *Communications in Nonlinear Science and Numerical Simulation.*, vol. 16, pp. 1874–1889, 2011.
- [22] M. S. Shadloo, A. Kimiaeifar, and D. Bagheri, “Series solution for heat transfer of continues stretching sheet immersed in a micropolar fluid in the existence of radiation,,” *International Journal of Numerical Methods for Heat and Fluid Flow.*, vol. 23, pp. 289–304, 2013.
- [23] D. Pal and S. Chatterjee, “Heat and mass transfer in mhd non-darcian flow of a micropolar fluid over a stretching sheet embedded in a porous media with non-uniform heat source and thermal radiation,” *Communications in Nonlinear Science and Numerical Simulation.*, vol. 15, pp. 1843–1857, 2010.
- [24] D. Pal and S. Chatterjee, “Effects of radiation on darcyforchheimer convective flow over a stretching sheet in a micropolar fluid with non-uniform heat source/sink,” *Journal of Applied Fluid Mechanics.*, vol. 8, pp. 207–212, 2015.

- [25] A. M. Subhas and N. Mahesha, "Heat transfer in mhd viscoelastic fluid flow over a stretching sheet with variable thermal conductivity, non-uniform heat source and radiation," *Applied Mathematical Modelling.*, vol. 32, pp. 1965–1983, 2008.
- [26] M. M. Rahman, M. J. Uddin, and A. Aziz, "Effects of variable electric conductivity and non-uniform heat source (or sink) on convective micropolar fluid flow along an inclined flat plate with surface heat flux," *International Journal of Thermal Sciences.*, vol. 48, pp. 2331–2340, 2009.
- [27] R. C. Bataller, "Viscoelastic fluid flow and heat transfer over a stretching sheet under the effects of a non-uniform heat source, viscous dissipation and thermal radiation," *International Journal of Heat and Mass Transfer*, vol. 50, no. 6, pp. 3152–3162, 2007.
- [28] M. I. Khan, M. Waqas, T. Hayat, and A. Alsaedi, "Soret and dufour effects in stretching flow of jeffrey fluid subject to newtonian heat and mass conditions," *Results in Physics*, vol. 7, pp. 4183–4188, 2017.
- [29] R. G. Mortimer and H. Eyring, "Elementary transition state theory of the soret and dufour effects," *Proceedings of the National Academy of Sciences of the United States of America.*, vol. 77, no. 4.
- [30] N. Ali, S. U. Khan, Z. Abbas, and M. Sajid, "Soret and dufour effects on hydromagnetic flow of viscoelastic fluid over porous oscillatory stretching sheet with thermal radiation," *Journal of the Brazilian Society of Mechanical Sciences and Engineering.*, vol. 38, no. 8.
- [31] T. Hayat, B. Ashraf, A. Alsaedi, and M. S. Alhuthali, "Soret and dufour effects in three-dimensional flow of maxwell fluid with chemical reaction and convective condition," *International Journal of Numerical Methods for Heat and Fluid Flow*, vol. 25, no. 1, pp. 98–120, 2015.
- [32] N. K. Singh, V. Kumar, and G. K. Sharma, "The effect of inclined magnetic field on unsteady flow past on moving vertical plate with variable temperature," *IJLTEMAS.*, vol. 5, no. 2, pp. 2278–2540, 2016.

- [33] G. S. Seth, R. Nandkeolyar, and M. S. Ansari, "Effects of hall current and rotation on unsteady mhd couette flow in the presence of an inclined magnetic field," *Journal of Applied Fluid Mechanics.*, vol. 5, no. 2, pp. 67–74, 2012.
- [34] A. A. Dar, "Effect of an inclined magnetic field on the flow of nano fluids in a tapered asymmetric porous chanal with heat source/sink and chemical reaction."
- [35] K. Momkos, "A comparison of the activation energy of viscous flow for hen egg-white lysozyme obtained on the basis of different models of viscosity for glass-forming liquids."
- [36] K. AbdulMaleque, "Effects of binary chemical reaction and activation energy on mhd boundary layer heat and mass transfer flow with viscous dissipation and heat generation/absorption."
- [37] M. Mustafa, J. A. Khan, T. Hayat, and A. Alsaedi, "Buoyancy effects on the mhd nanofluid flow past a vertical surface with chemical reaction and activation energy."
- [38] F. Mabood, S. M. Ibrahim, M. M. Rashidi, M. S. Shadloo, and G. Lorenzini, "Non-uniform heat source/sink and solet effects on mhd non-darcian convective flow past a stretching sheet in a micropolar fluid with radiation," *International Journal of Heat and Mass Transfer.*, vol. 93, p. 674682, 2016.
- [39] Y. A. Cengel and J. M. Cimbala, "Fluid mechanics," p. 931, 2006.
- [40] D. J. Tritton, "Physical fluid dynamics," p. 346., 1977.
- [41] S. MOLOKOV, R. MOREAU, and H. K. MOFFATT, "Magnetohydrodynamics, historical evolution and trends," *Book*, p. p 407, 2006.
- [42] B. Massey and J. Ward-Smith, "Mechanics of fluids," p. 689, 2006.
- [43] C. P. Kothandaraman, "Fundamentals of haet and mass transfer," p. 712, 2006.
- [44] A. J. Smits, "A physical introduction to fluid mechanics," p. 321, 2018.

-
- [45] J. Kunes., “Dimensionless physical quantities in science and engineering,” *Book*, p. p 441, 2012.
- [46] M. Qasim, I. Khan, and S. Shafie, “Heat transfer in a micropolar fluid over a stretching sheet with newtonian heating,” *PLoS ONE*, vol. 8, no. 4.
- [47] L. G. Grubka and K. M. Bobba, “Heat transfer characteristics of a continuous stretching surface with variable temperature,” *Journal of Heat Transfer*, vol. 1074, pp. 248–250, 1985.
- [48] C. K. Chen and M. I. Char, “Heat transfer of a continuous stretching surface with suction or blowing,” *Journal of Mathematical Analysis and Applications*, vol. 135, no. 2, pp. 568–580, 1988.